Design Strategies for Enhancing Gas Separation with High-Performance Mixed Matrix Membranes

Mehdi Ghasemi, Lev Sarkisov, Masoud Babaei

Department of Chemical Engineering, The University of Manchester

8th Post-Combustion Capture Conference

September 2025

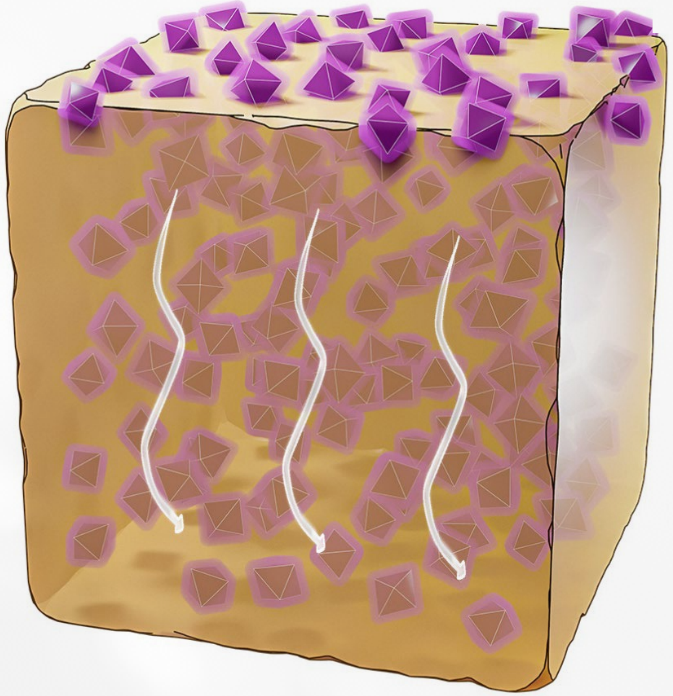

Overview

Research Statement

Methodology

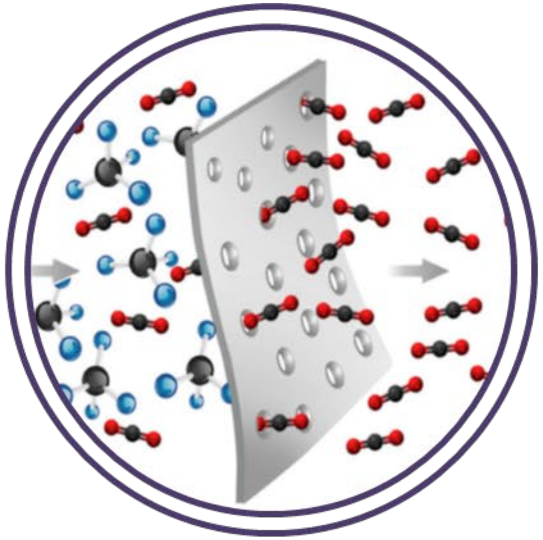

Results & Discussion

Overview

Research Statement

Membrane Technology

Gas Mixture Separation

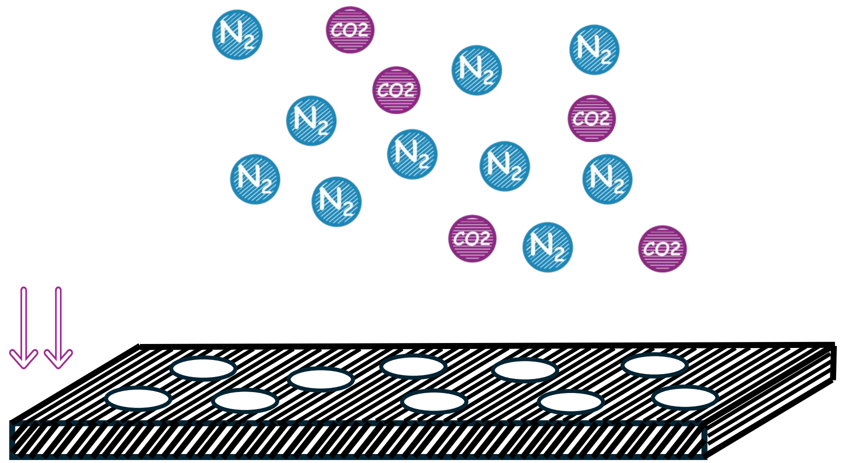

- **Pros**:
  Operative flexibility
  Low energy cost

- **Cons:**
  Need of materials in high performance

Performance Evaluation

- Permeability

$$P_i = D_i \times S_i$$

Diffusion Coefficient

Solubility Coefficient

- Selectivity

$$\alpha_{ij} = \frac{P_i}{P_j} = (\frac{D_i}{D_j}) \times (\frac{S_i}{S_j})$$

Kinetics-driven

Sorption-driven

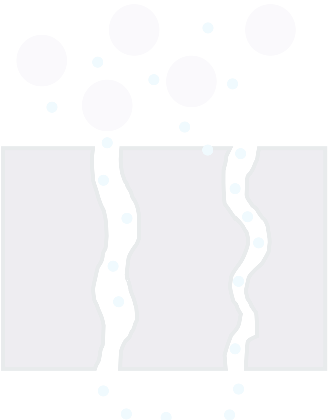

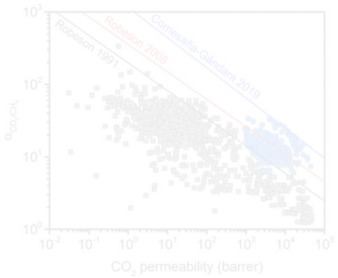

Membrane Technology

Gas Mixture Separation

- **Pros:**
  Operative flexibility
  Low energy cost
- **Cons:**
  Need of materials in high performance

Performance Evaluation

- Permeability

$$P_i = \boxed{D_i} \times \boxed{S_i}$$

Diffusion Coefficient

Solubility Coefficient

- Selectivity

$$\alpha_{ij} = \frac{P_i}{P_j} = \boxed{\left(\frac{D_i}{D_j}\right)} \times \boxed{\left(\frac{S_i}{S_j}\right)}$$

Kinetics-driven

Sorption-driven

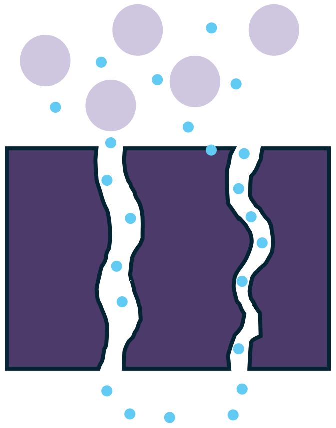

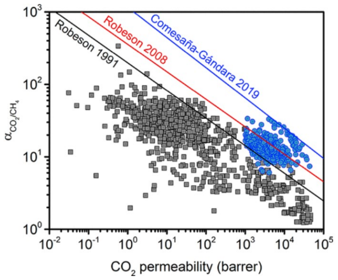

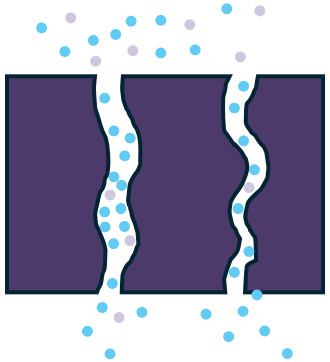

Membrane Technology

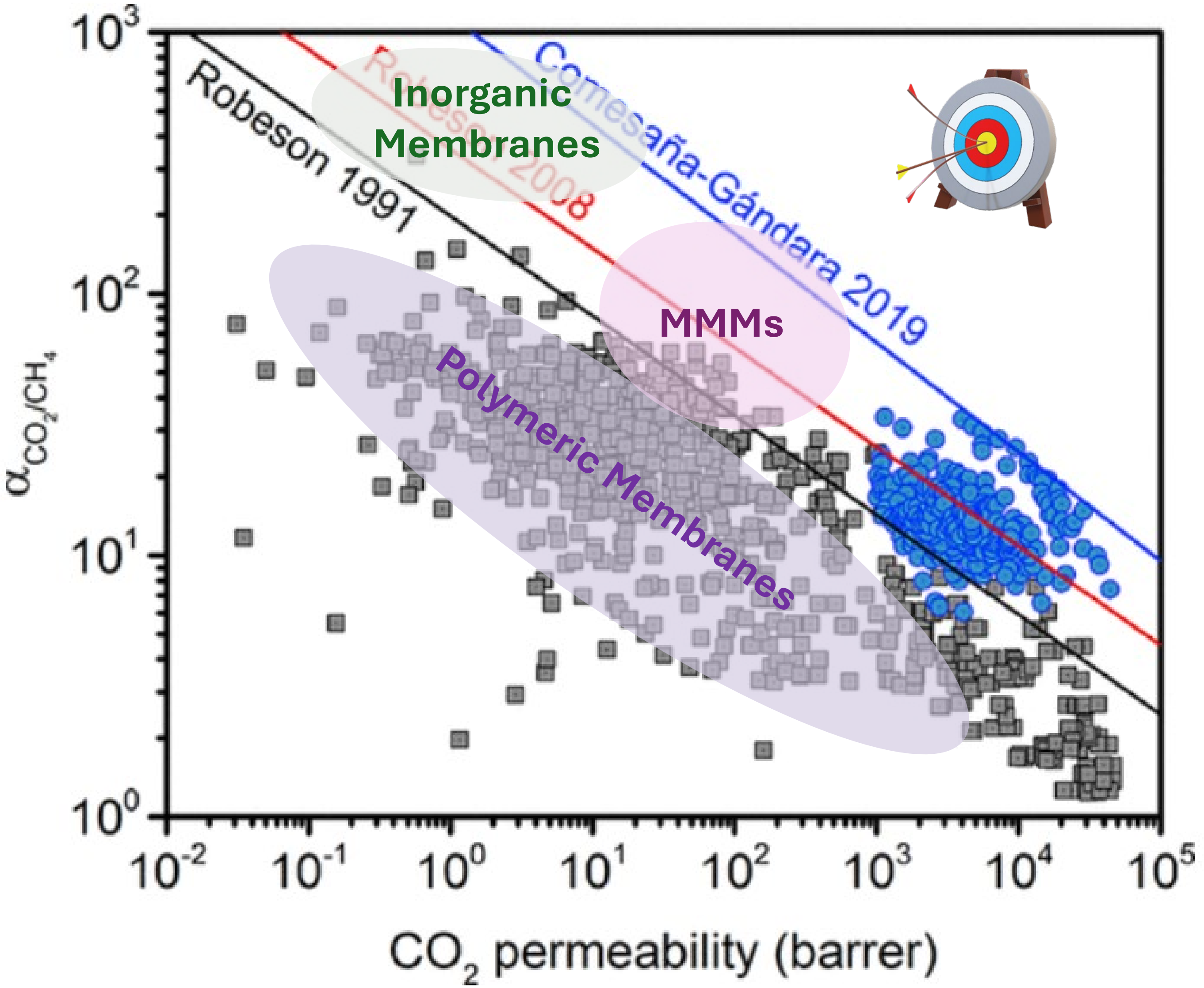

Upper bound plot for CO_2/CH_4 for homogeneous, solution-processable polymeric materials. [*Qian et al. 2020*]

Overview

Research Statement

Overview

Research Statement

Methodol

Research Statement

Material Desing

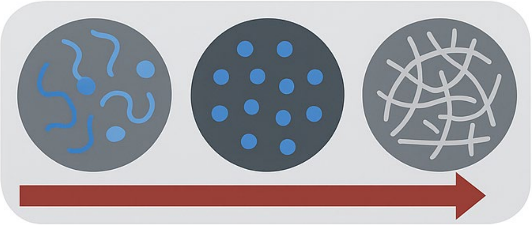

Permeability and Selectivity

Membrane

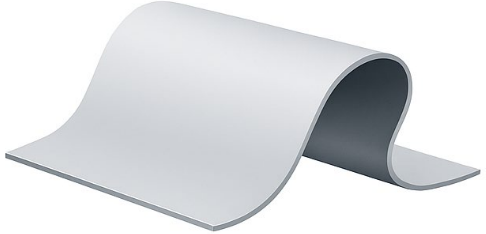

Permeance

Membrane Device

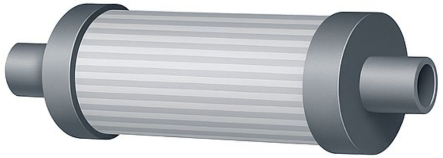

Module type

Membrane Process

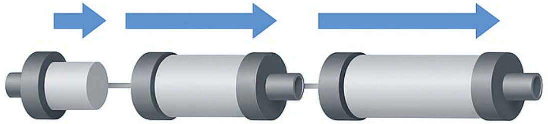

Optimal process

How to improve Permselectivity in MMMs?

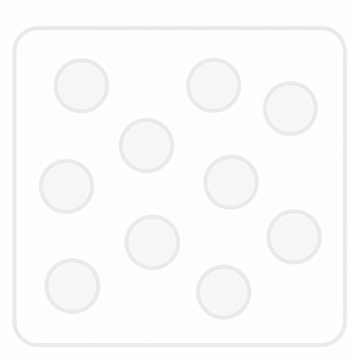

Filler arrangements

Interfacial compatibility

Filler Shape

Filler Loading

Research Statement

Material Desing

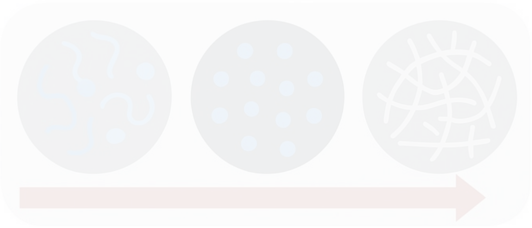

Permeability and Selectivity

Membrane

Permeance

Membrane Device

Module type

Membrane Process

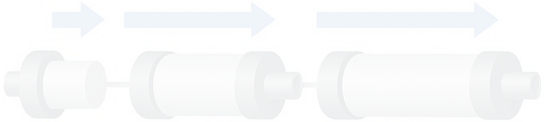

Optimal process

How to improve Permselectivity in MMMs?

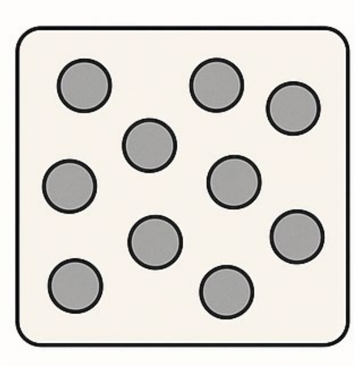

Filler arrangements

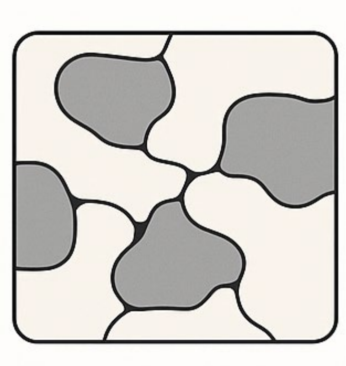

Interfacial compatibility

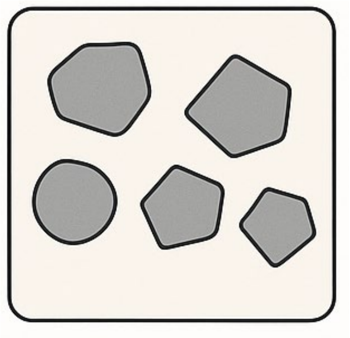

Filler Shape

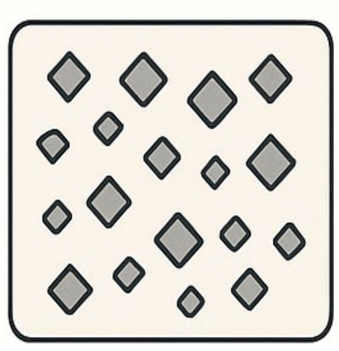

Filler Loading

Research Statement

To what extent can filler shapes influence permselectivity?

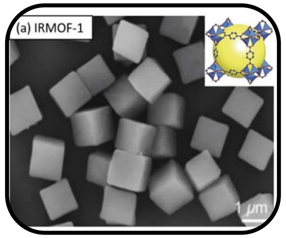

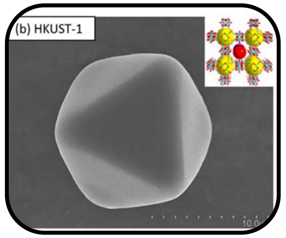

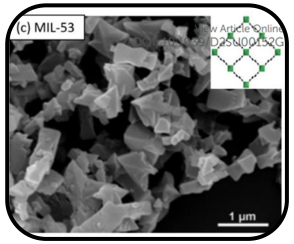

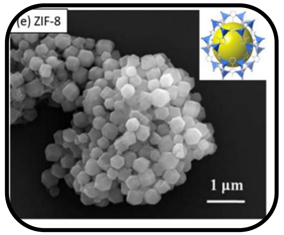

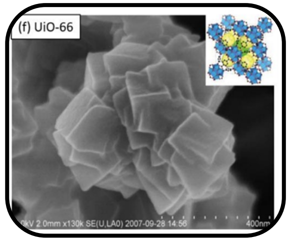

Metal–**O**rganic **F**rameworks **(MOFs)**, **C**ovalent–**O**rganic **F**rameworks **(COFs)**, **M**etal–**O**rganic **P**olyhedra **(MOPs)**

How do the intricate relationships between the geometrical features of interfacial defects and the arrangements of filler particles influence permselectivity?

Research Statement

To what extent can filler shapes influence permselectivity?

Metal–Organic Frameworks **(MOFs)**, Covalent–Organic Frameworks **(COFs)**, Metal–Organic Polyhedra **(MOPs)**

How do the intricate relationships between the geometrical features of interfacial defects and the arrangements of filler particles influence permselectivity?

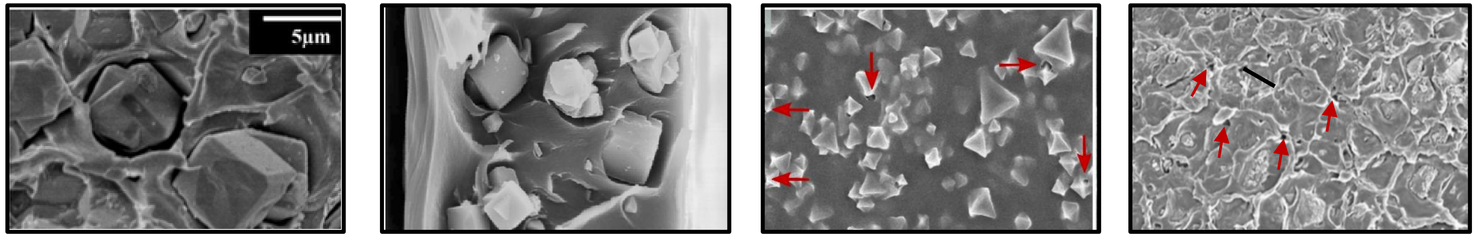

Overview

Research Statement

Methodol

Research
tatement

Methodology

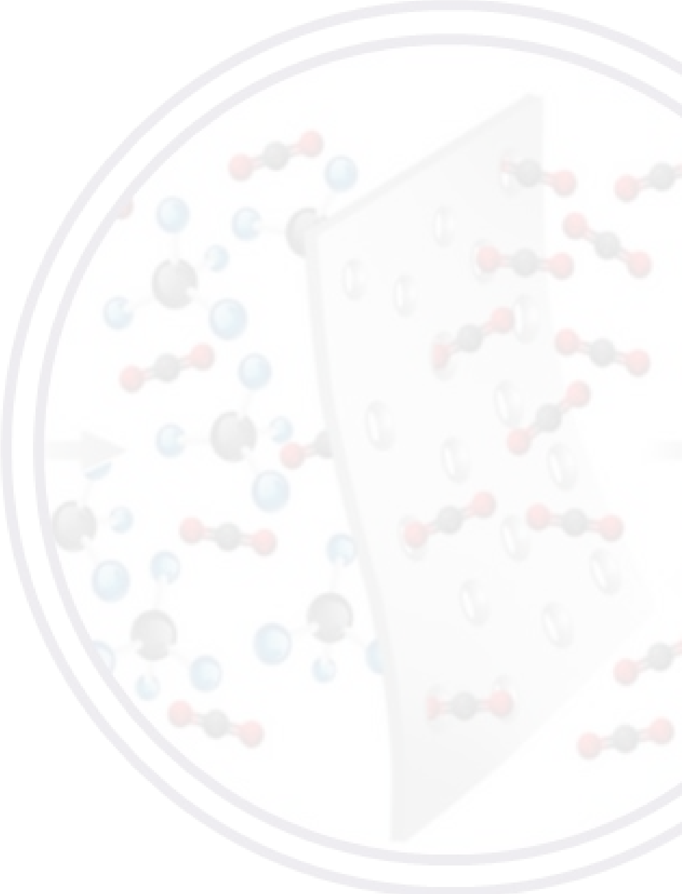

Results
Discussi

Methodology

Structure generation

- Geometric expressions of particle
  - Sets of edges, faces, and vertices.

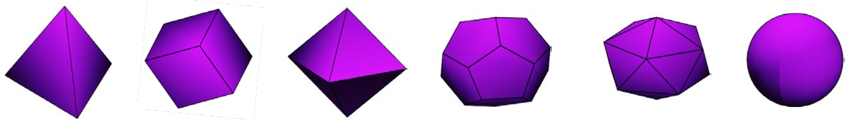

  - Voxel-based particle representation

resolution-dependent nature!

How to ensure about the resolution?

D_{eq} :diameter of a sphere equivalent in volume to a Platonic particle

Resolution: length of voxel/D_{eq}

- Distribution algorithm

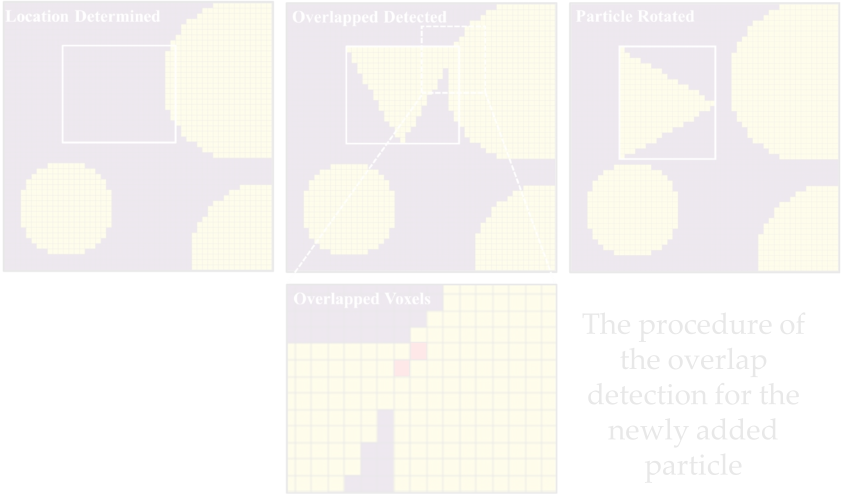

The procedure of the overlap detection for the newly added particle

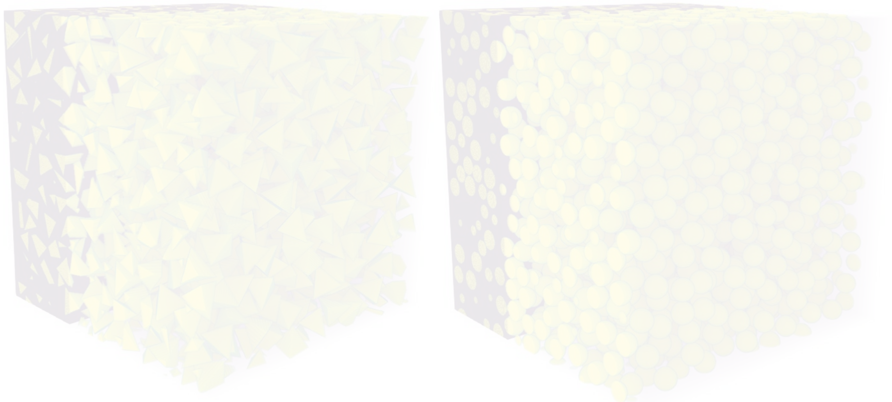

Illustrations of the digitized membrane domain

Methodology

Structure generation

Geometric expressions of particle

- Sets of edges, faces, and vertices.

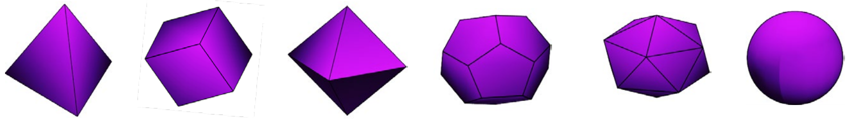

Tetrahedron	Hexahedron	Octahedron	Dodecahedron	Icosahedron	Sphere
s = 0.67	s = 0.81	s = 0.84	s = 0.91	s = 0.94	s = 1

- Voxel-based particle representation

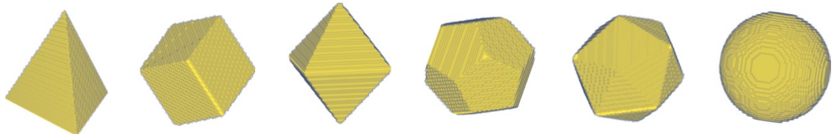

resolution-dependent nature!

How to ensure about the resolution?

D_{eq} :diameter of a sphere equivalent in volume to a Platonic particle

Resolution: length of voxel/D_{eq}

Distribution algorithm

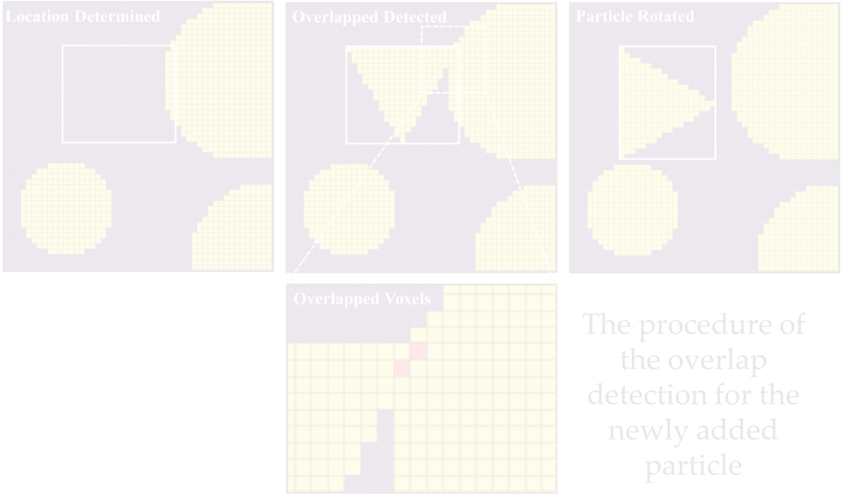

The procedure of the overlap detection for the newly added particle

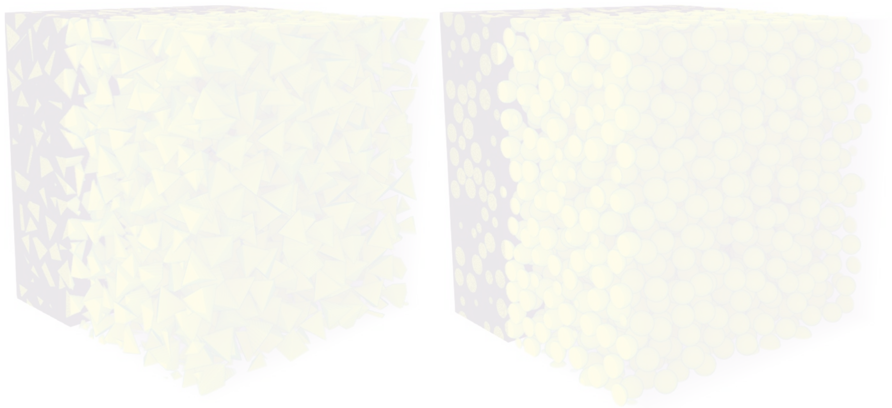

Illustrations of the digitized membrane domain

Methodology

Structure generation

- Geometric expressions of particle
  - Sets of edges, faces, and vertices.

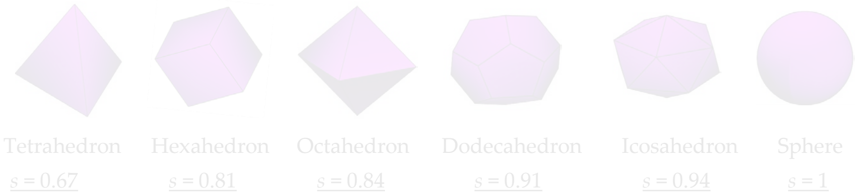

  - Voxel-based particle representation

resolution-dependent nature!

How to ensure about the resolution?

D_{eq} :diameter of a sphere equivalent in volume to a Platonic particle

Resolution: length of voxel/D_{eq}

- Distribution algorithm

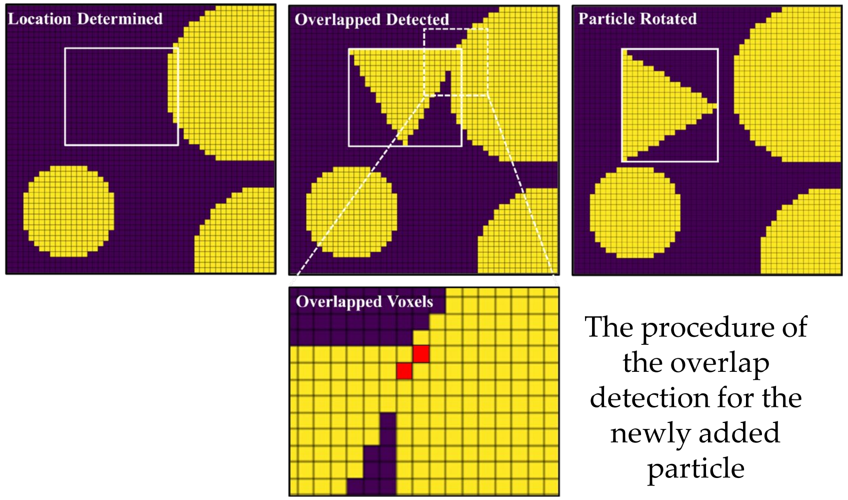

The procedure of the overlap detection for the newly added particle

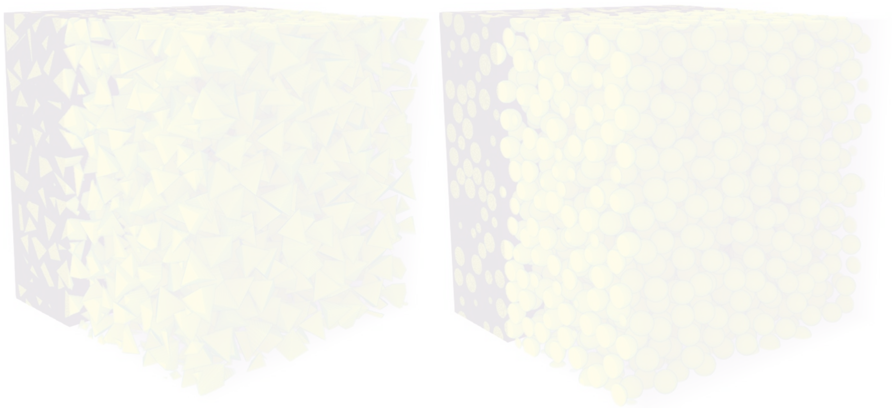

Illustrations of the digitized membrane domain

Methodology

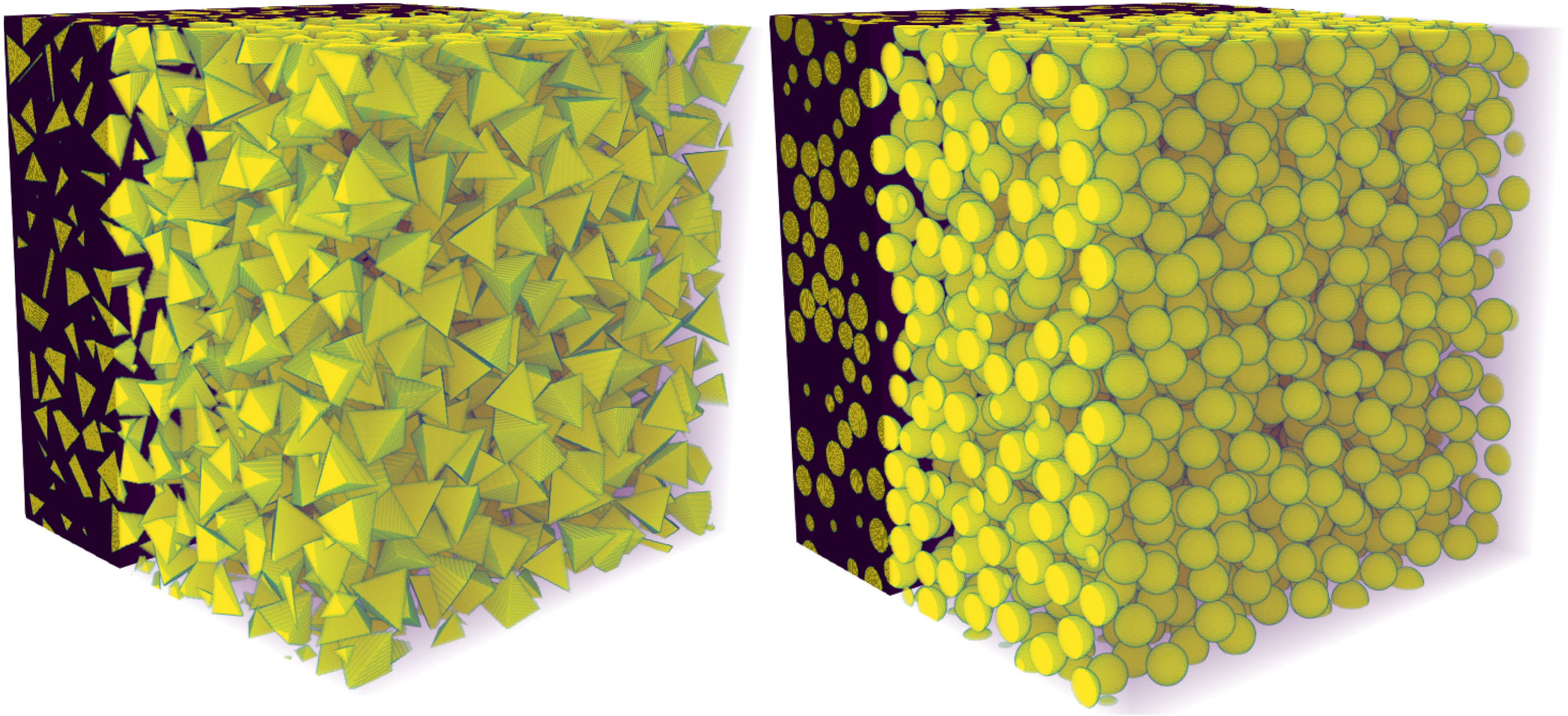

Methodology

- Filler particles with interfacial defect

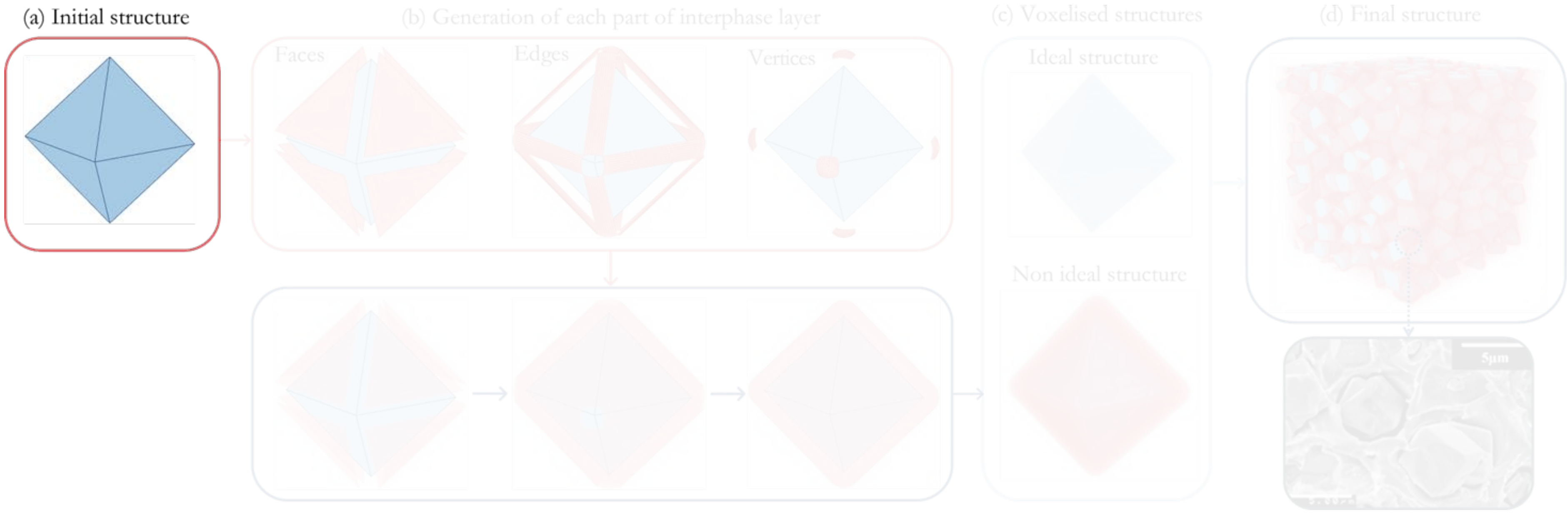

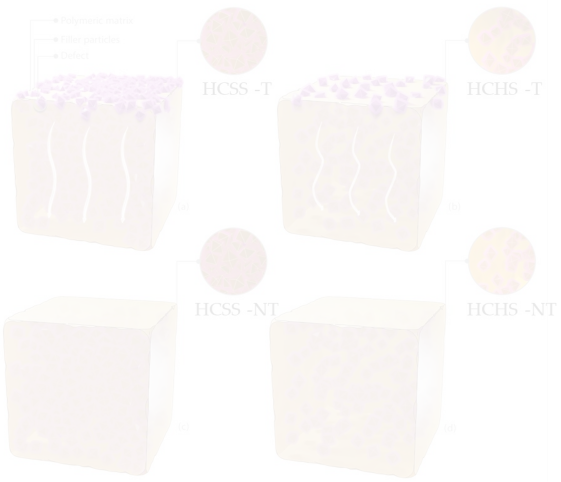

Methodology

- Filler particles with interfacial defect

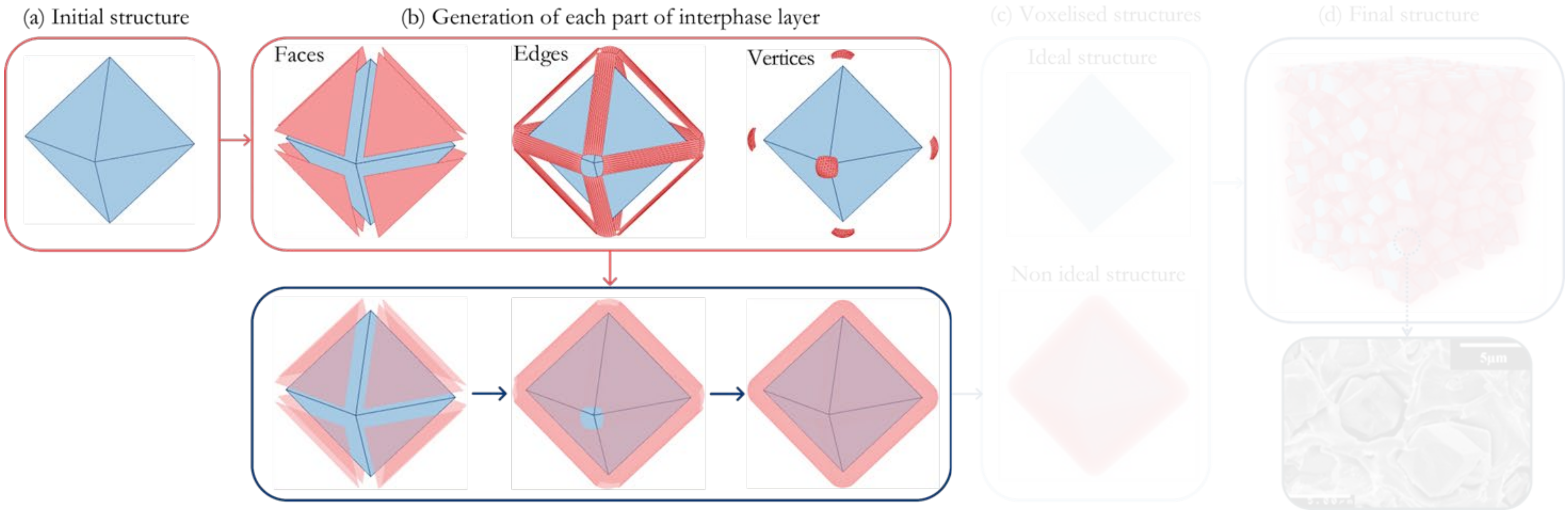

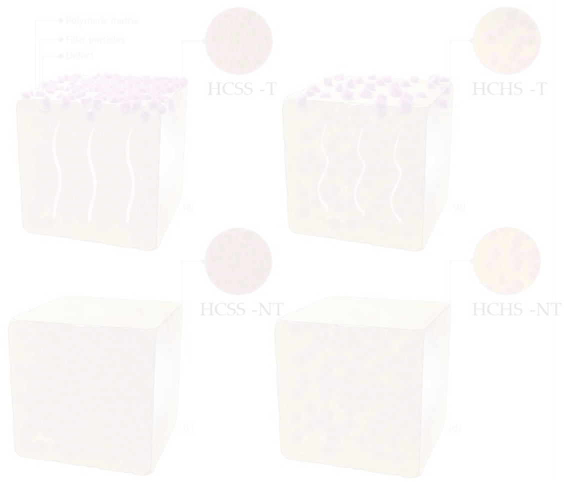

Methodology

- Filler particles with interfacial defect

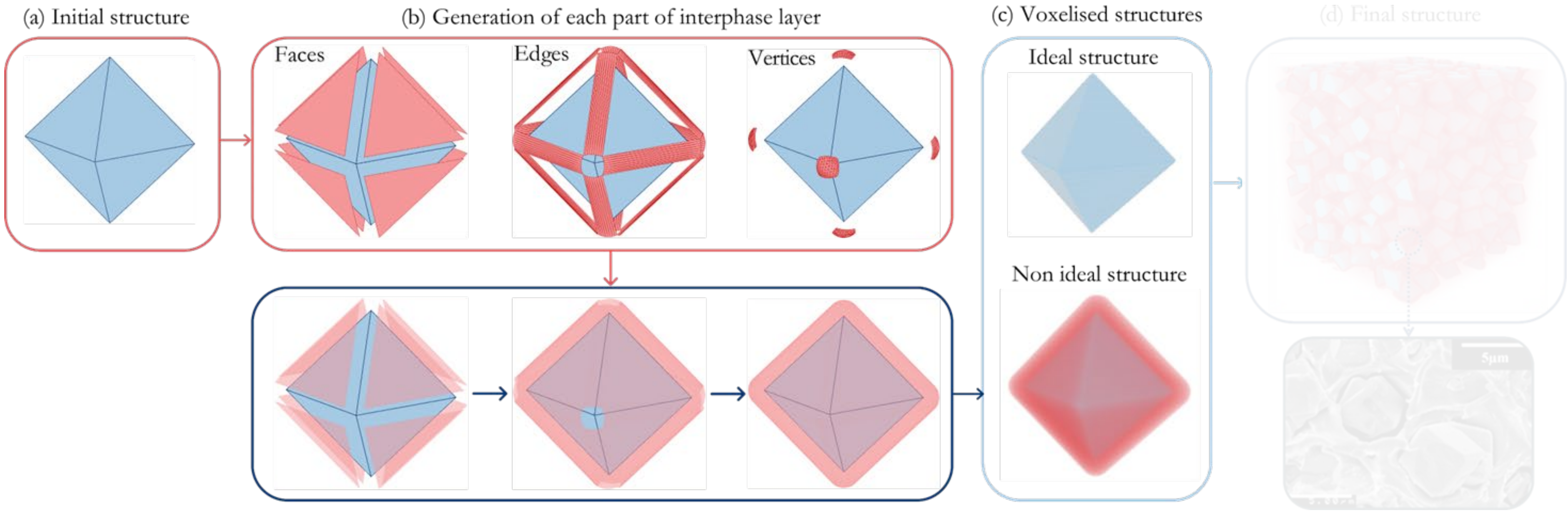

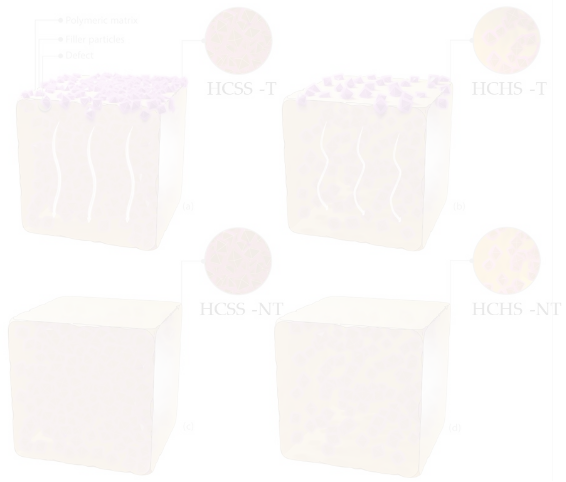

Methodology

- Filler particles with interfacial defect

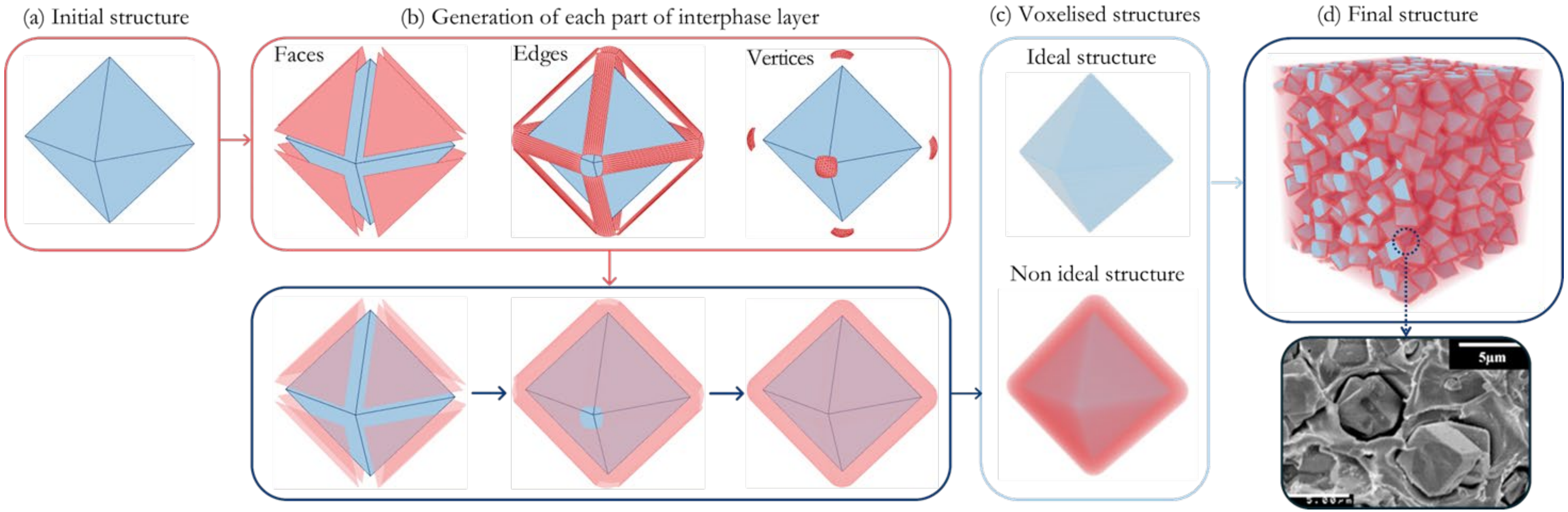

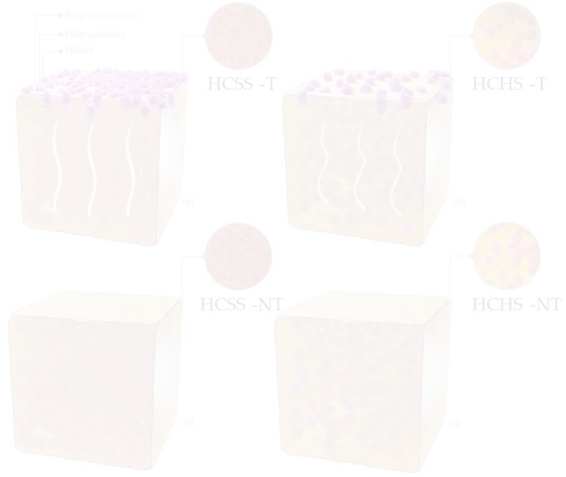

Methodology

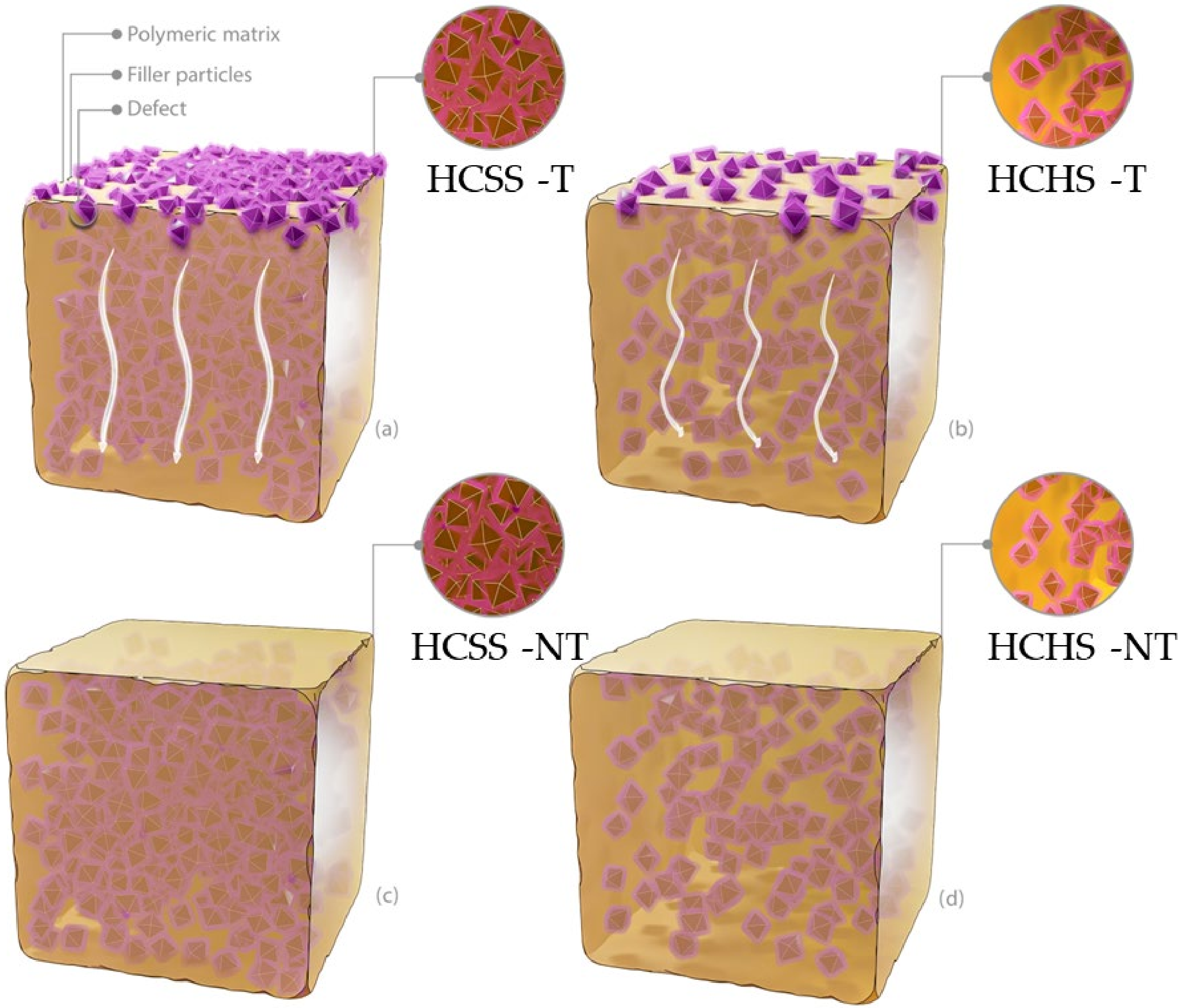

Methodology

- The Maxwell Stephan transport model

$$-\rho \frac{\theta_i}{RT}\nabla\mu_i = \sum_{j=1}^{n} \frac{q_j J_i - q_i J_j}{q_i^{sat} q_j^{sat} D_{ij}} + \frac{J_i}{q_i^{sat} D_i}$$

- Under weak confinement scenario

$$-J_i = \underbrace{\rho q_{isat} D_i \frac{\theta_i}{p_i}}_{P_i} \nabla p_i$$

$$J_{i,r} = \sum_j -P_{i,j}\left(\frac{\partial p_i}{\partial r}\right) + J_{j,MD}$$

Phases

Diffusion correction for the gas mixture

$$J_{j,MD} = \frac{\sum_i M_i P_{i,j} \frac{\partial p}{\partial r}}{M}, \quad \frac{1}{M} = \sum_i \frac{1}{M_i}$$

Inlet side

$$p_1 = p_2 = \frac{1}{2} p_{inlet}$$

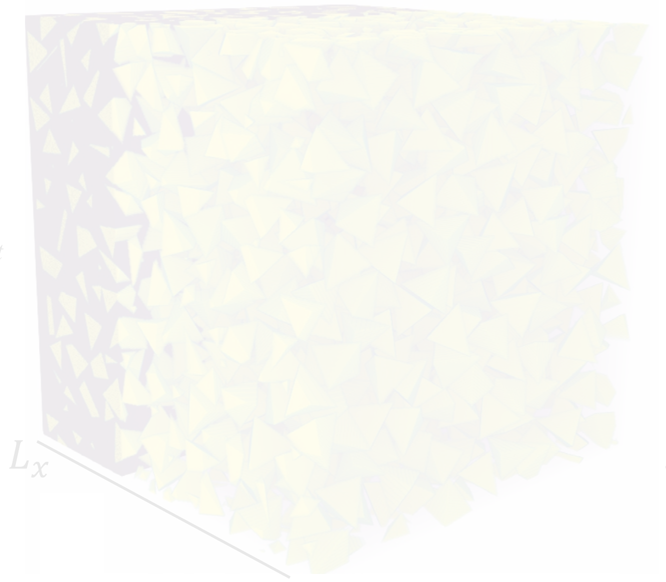

Outlet side

$$p_1 + p_2 = p_{outlet}$$

$$\frac{J_{1,x}}{J_{2,x}} = \frac{p_1}{p_2}$$

$$P_{i,MMM} = \frac{J_{i,x}.L_x}{\Delta p_i}$$

$$J_{i,x} = \frac{1}{L_y L_z}\iint_S J_i(x,y,z)\,dydz$$

$$\alpha_{MMM} = \frac{J_{1,x}}{J_{2,x}}$$

Methodology

- The Maxwell Stephan transport model

$$-\rho \frac{\theta_i}{RT} \nabla \mu_i = \sum_{j=1}^{n} \frac{q_j J_i - q_i J_j}{q_i^{sat} q_j^{sat} D_{ij}} + \frac{J_i}{q_i^{sat} D_i}$$

- Under weak confinement scenario

$$-J_i = \underbrace{\rho q_{isat} D_i \frac{\theta_i}{p_i}}_{P_i} \nabla p_i$$

$$J_{i,r} = \sum_{j} -P_{i,j} \left(\frac{\partial p_i}{\partial r} \right) + J_{j,MD}$$

Phases

Diffusion correction for the gas mixture

$$J_{j,MD} = \frac{\sum_i M_i P_{i,j} \frac{\partial p}{\partial r}}{M}, \quad \frac{1}{M} = \sum_i \frac{1}{M_i}$$

Inlet side

$$p_1 = p_2 = \frac{1}{2} p_{inlet}$$

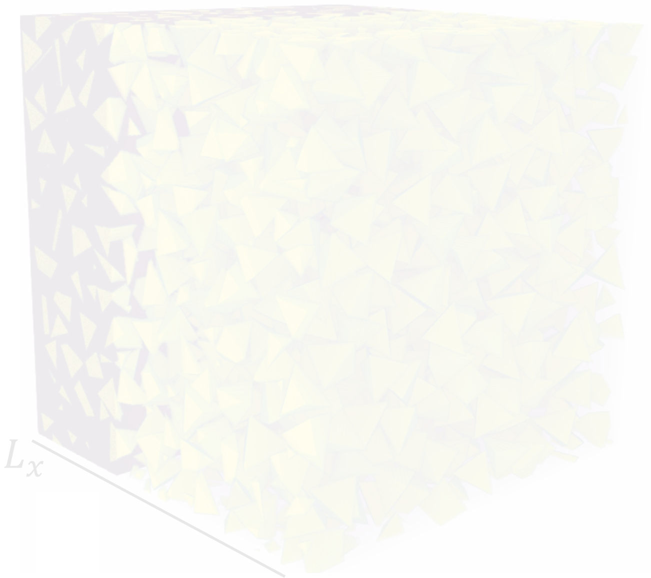

Outlet side

$$p_1 + p_2 = p_{outlet}$$

$$\frac{J_{1,x}}{J_{2,x}} = \frac{p_1}{p_2}$$

$$P_{i,MMM} = \frac{J_{i,x} . L_x}{\Delta p_i}$$

$$J_{i,x} = \frac{1}{L_y L_z} \iint_S J_i(x, y, z) dydz$$

$$\alpha_{MMM} = \frac{J_{1,x}}{J_{2,x}}$$

Methodology

- The Maxwell Stephan transport model

$$-\rho \frac{\theta_i}{RT} \nabla \mu_i = \sum_{j=1}^{n} \frac{q_j J_i - q_i J_j}{q_i^{sat} q_j^{sat} D_{ij}} + \frac{J_i}{q_i^{sat} D_i}$$

- Under weak confinement scenario

$$-J_i = \underbrace{\rho q_{isat} D_i \frac{\theta_i}{p_i}}_{P_i} \nabla p_i$$

$$J_{i,r} = \sum_j -P_{i,j} \left(\frac{\partial p_i}{\partial r} \right) + J_{j,MD}$$

Phases

Diffusion correction for the gas mixture

$$J_{j,MD} = \frac{\sum_i M_i P_{i,j} \frac{\partial p}{\partial r}}{M}, \quad \frac{1}{M} = \sum_i \frac{1}{M_i}$$

Inlet side

$$p_1 = p_2 = \frac{1}{2} p_{inlet}$$

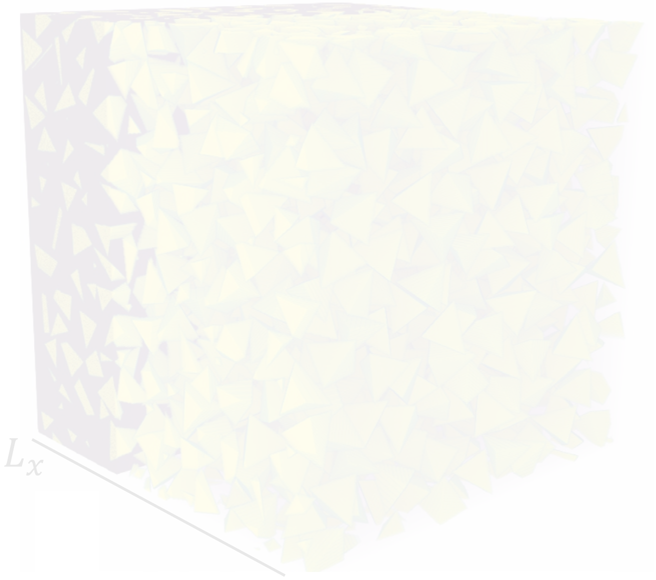

Outlet side

$$p_1 + p_2 = p_{outlet}$$

$$\frac{J_{1,x}}{J_{2,x}} = \frac{p_1}{p_2}$$

$$P_{i,MMM} = \frac{J_{i,x} . L_x}{\Delta p_i}$$

$$J_{i,x} = \frac{1}{L_y L_z} \iint_S J_i(x, y, z) dydz$$

$$\alpha_{MMM} = \frac{J_{1,x}}{J_{2,x}}$$

Methodology

- The Maxwell Stephan transport model

$$-\rho \frac{\theta_i}{RT} \nabla \mu_i = \sum_{j=1}^{n} \frac{q_j J_i - q_i J_j}{q_i^{sat} q_j^{sat} D_{ij}} + \frac{J_i}{q_i^{sat} D_i}$$

- Under weak confinement scenario

$$-J_i = \underbrace{\rho q_{isat} D_i \frac{\theta_i}{p_i}}_{P_i} \nabla p_i$$

$$J_{i,r} = \sum_{j} -P_{i,j} \left(\frac{\partial p_i}{\partial r} \right) + J_{j,MD}$$

Phases

Diffusion correction for the gas mixture

$$J_{j,MD} = \frac{\sum_i M_i P_{i,j} \frac{\partial p}{\partial r}}{M}, \quad \frac{1}{M} = \sum_i \frac{1}{M_i}$$

Inlet side

$$p_1 = p_2 = \frac{1}{2} p_{inlet}$$

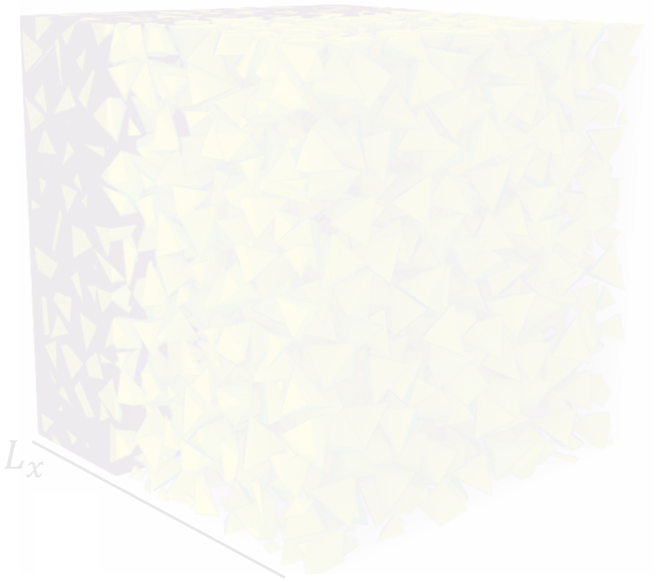

Outlet side

$$p_1 + p_2 = p_{outlet}$$

$$\frac{J_{1,x}}{J_{2,x}} = \frac{p_1}{p_2}$$

$$P_{i,MMM} = \frac{J_{i,x} . L_x}{\Delta p_i}$$

$$J_{i,x} = \frac{1}{L_y L_z} \iint_S J_i(x, y, z) dydz$$

$$\alpha_{MMM} = \frac{J_{1,x}}{J_{2,x}}$$

Methodology

- The Maxwell Stephan transport model

$$-\rho \frac{\theta_i}{RT}\nabla\mu_i = \sum\nolimits_{j=1}^{n} \frac{q_j J_i - q_i J_j}{q_i^{sat} q_j^{sat} D_{ij}} + \frac{J_i}{q_i^{sat} D_i}$$

- Under weak confinement scenario

$$-J_i = \underbrace{\rho q_{isat} D_i \frac{\theta_i}{p_i}}_{P_i} \nabla p_i$$

Inlet side

$$p_1 = p_2 = \frac{1}{2} p_{inlet}$$

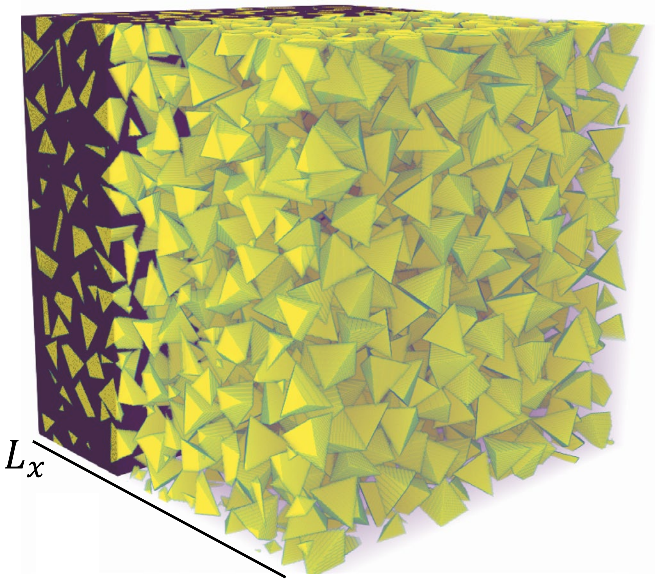

Outlet side

$$p_1 + p_2 = p_{outlet}$$

$$\frac{J_{1,x}}{J_{2,x}} = \frac{p_1}{p_2}$$

$$J_{i,r} = \sum_{j} -P_{i,j}\left(\frac{\partial p_i}{\partial r}\right) + J_{j,MD}$$

Phases

Diffusion correction for the gas mixture

$$P_{i,MMM} = \frac{J_{i,x}.L_x}{\Delta p_i}$$

$$J_{i,x} = \frac{1}{L_y L_z}\iint_S J_i(x,y,z)dydz$$

$$\alpha_{MMM} = \frac{J_{1,x}}{J_{2,x}}$$

$$J_{j,MD} = \frac{\sum_i M_i P_{i,j} \frac{\partial p}{\partial r}}{M}, \quad \frac{1}{M} = \sum_i \frac{1}{M_i}$$

Methodology

- The Maxwell Stephan transport model

$$-\rho \frac{\theta_i}{RT}\nabla\mu_i = \sum_{j=1}^{n} \frac{q_j J_i - q_i J_j}{q_i^{sat} q_j^{sat} D_{ij}} + \frac{J_i}{q_i^{sat} D_i}$$

- Under weak confinement scenario

$$-J_i = \underbrace{\rho q_{isat} D_i \frac{\theta_i}{p_i}}_{P_i} \nabla p_i$$

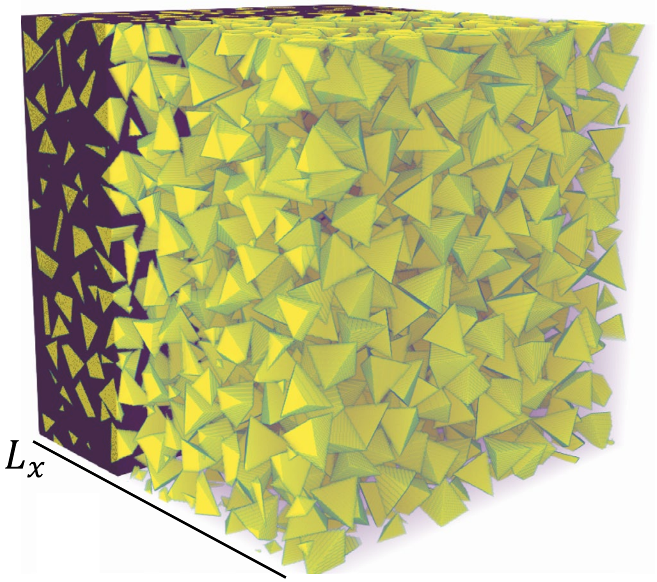

Inlet side

$$p_1 = p_2 = \frac{1}{2} p_{inlet}$$

Outlet side

$$p_1 + p_2 = p_{outlet}$$

$$\frac{J_{1,x}}{J_{2,x}} = \frac{p_1}{p_2}$$

$$J_{i,r} = \sum_j -P_{i,j}\left(\frac{\partial p_i}{\partial r}\right) + J_{j,MD}$$

Phases

Diffusion correction for the gas mixture

$$J_{j,MD} = \frac{\sum_i M_i P_{i,j} \frac{\partial p}{\partial r}}{M}, \quad \frac{1}{M} = \sum_i \frac{1}{M_i}$$

$$P_{i,MMM} = \frac{J_{i,x}.L_x}{\Delta p_i}$$

$$J_{i,x} = \frac{1}{L_y L_z} \iint_S J_i(x,y,z)\,dydz$$

$$\alpha_{MMM} = \frac{J_{1,x}}{J_{2,x}}$$

Research
tatement

Methodology

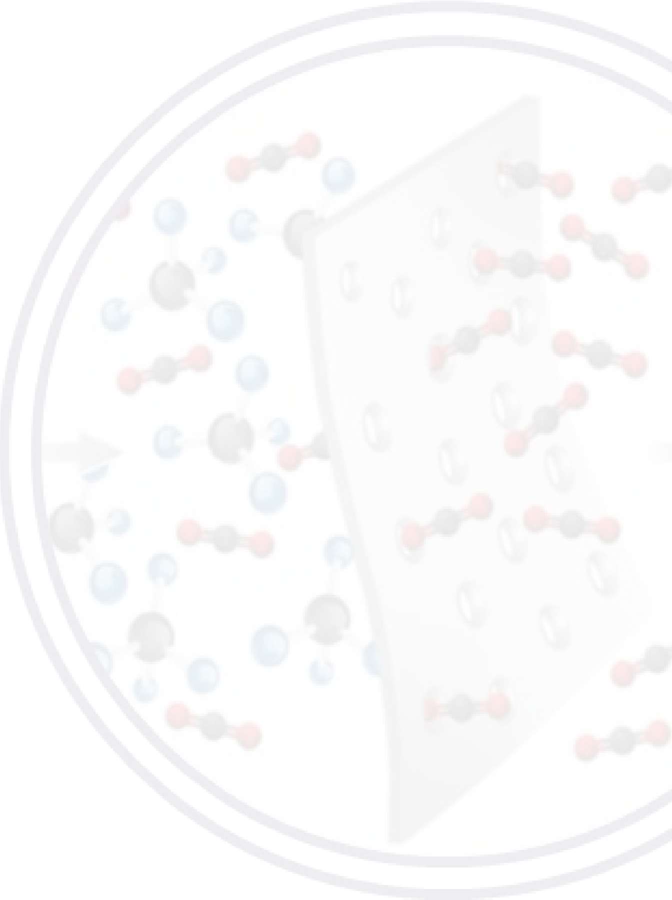

Results
Discussi

thodology

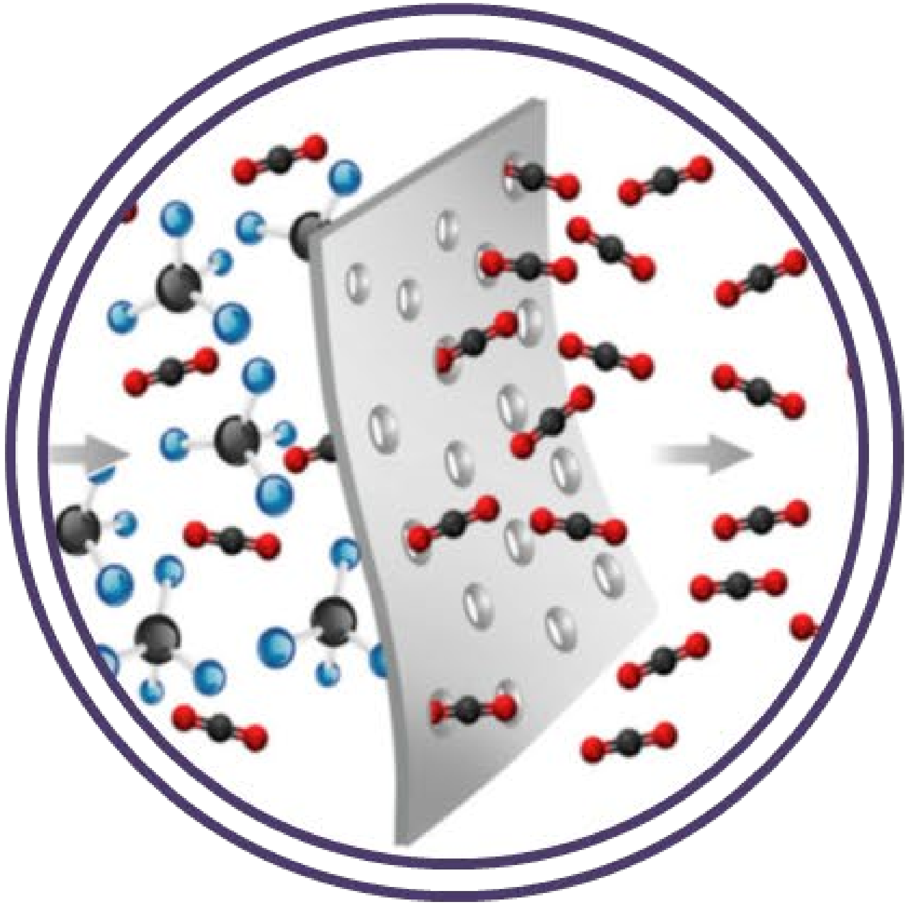

Results & Discussion

Results & Discussion

Validation of the model

- Impact of resolution: 8, 10, and 16 pixels/nm
- Impact of REV: 240, 300, and 400 pixels

↓

<u>R8 and REV300</u>

In comparison with analytical models?

- Up to 15% loading, all have the same behaviours.
- Relative errors:

Bruggeman: 1.43%

Cheiw-Glandt: 5.17%

Pal: 10.32%

Maxwell:14.25%

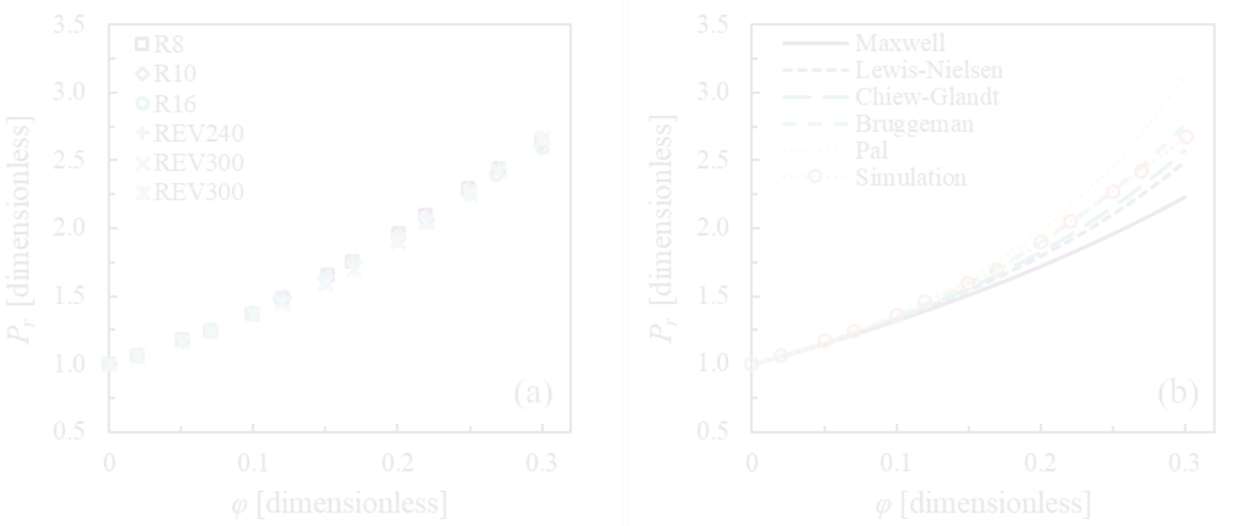

(a) Assessing the influence of three different resolutions (nm/pixel) as well as the impacts of REV on the predicted permeability. (b) Comparison of our models with the analytical models. For part (a), all simulation are conducted for P_i/P_m=100 and ϕ = 20%.

Results & Discussion

Validation of the model

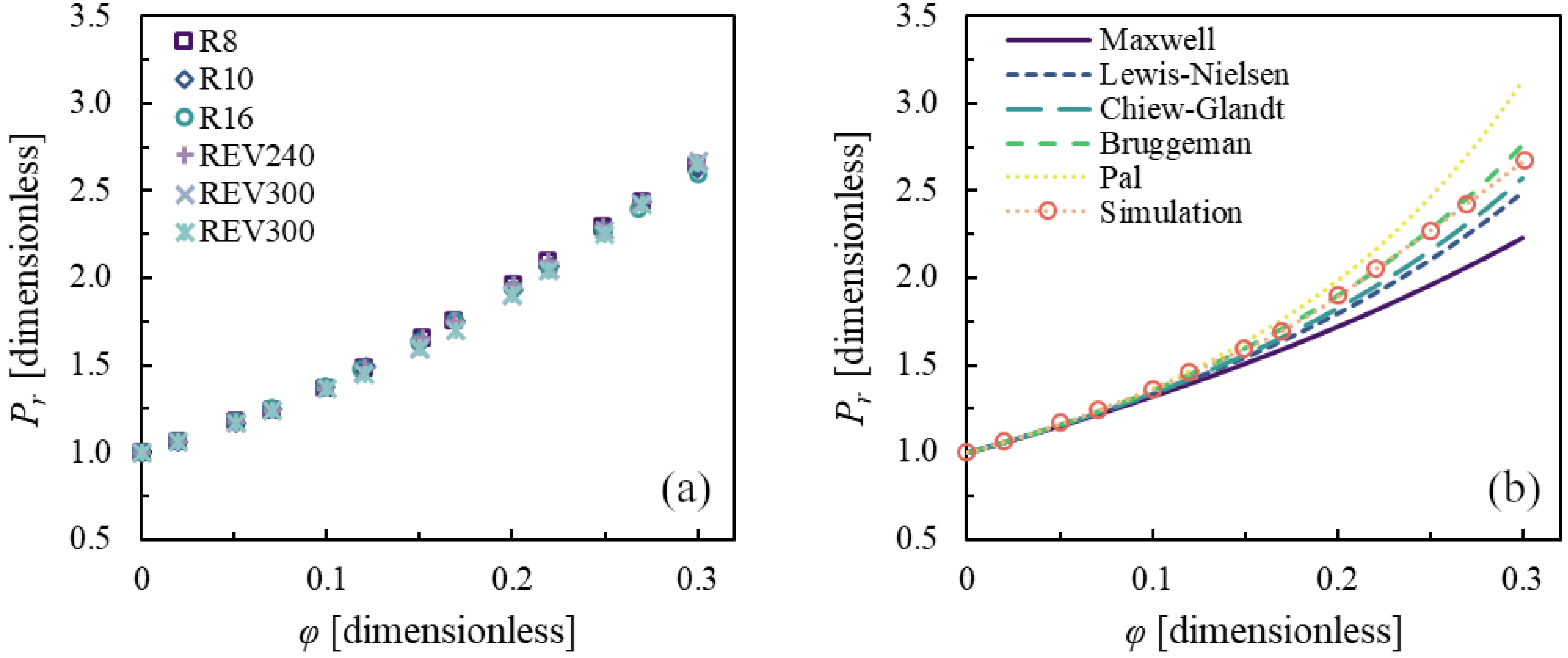

(a) Assessing the influence of three different resolutions (nm/pixel) as well as the impacts of REV on the predicted permeability. (b) Comparison of our models with the analytical models. For part (a), all simulation are conducted for P_f $/P_m$=100 and ϕ = 20%.

Results & Discussion

Ideal MMMs

- Impact of particle shape
- Impact of loading
- Impact of filler to polymer permeability ratio

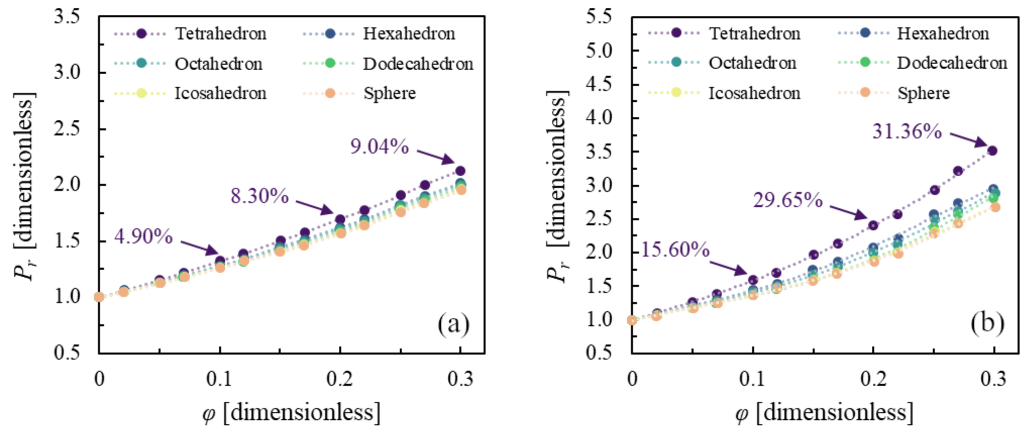

The impact of loading fractions, ϕ on the permeability of the MMM containing filler particles with a Platonic structure, as compared to spherical particles, for P_f/P_m is equal to (a) 10 and (b) 100.

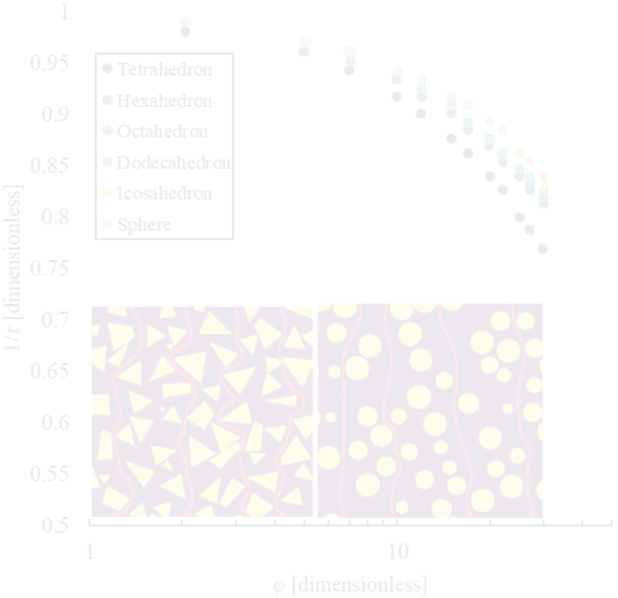

Comparison of the inverse of tortuosity (1/τ) of Platonic particles and spheres for loading fractions obtained by open-source MATLAB code, TauFactor [14].

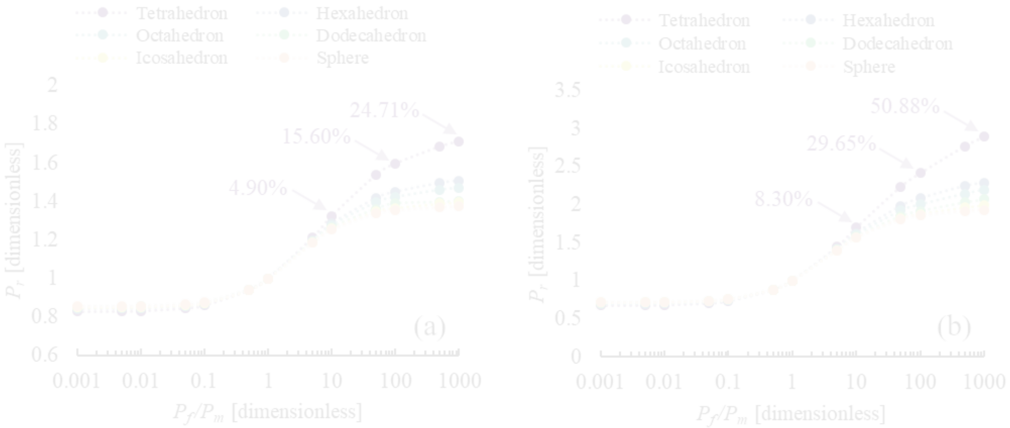

The impact of filler permeability relative to the polymer permeability, P_f/P_m, on the permeability of MMM for loading fraction, ϕ equal to (a) 10% and (b) 20%.

Results & Discussion

Ideal MMMs

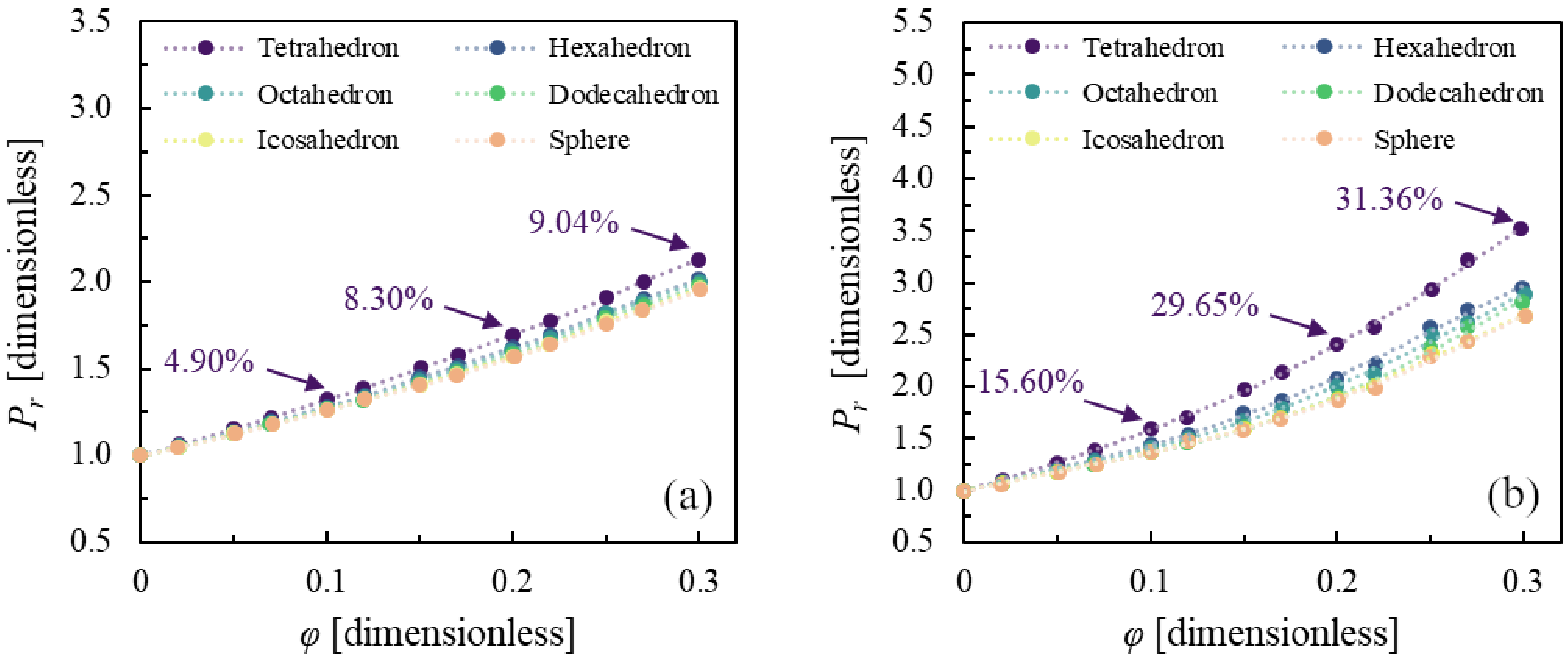

The impact of loading fractions, ϕ on the permeability of the MMM containing filler particles with a Platonic structure, as compared to spherical particles, for P_f/P_m is equal to (a) 10 and (b) 100.

Results & Discussion

Ideal MMMs

- Impact of particle shape
- Impact of loading
- Impact of filler to polymer permeability ratio

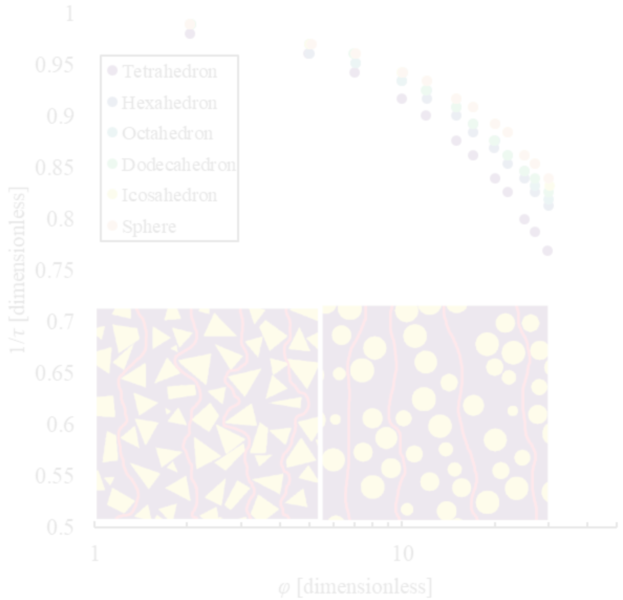

Comparison of the inverse of tortuosity (1/τ) of Platonic particles and spheres for loading fractions obtained by open-source MATLAB code, TauFactor [14].

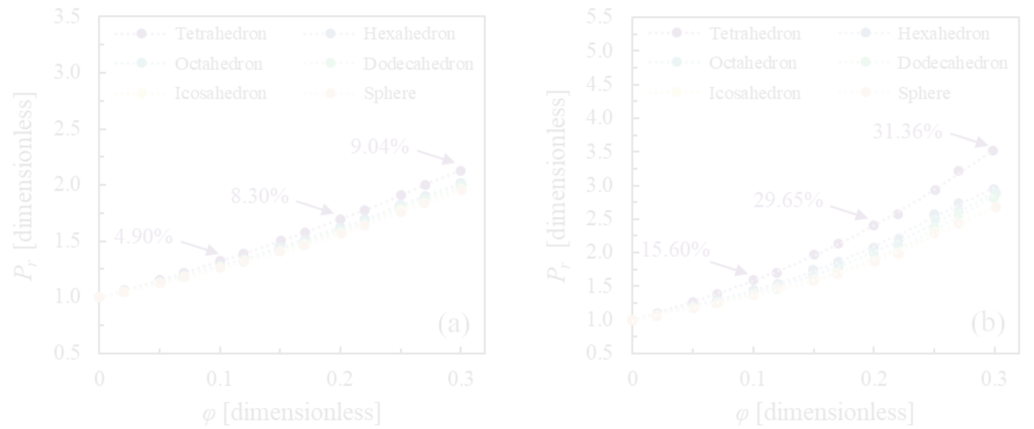

The impact of loading fractions, ϕ on the permeability of the MMM containing filler particles with a Platonic structure, as compared to spherical particles, for *P*f /*P*m is equal to (a) 10 and (b) 100.

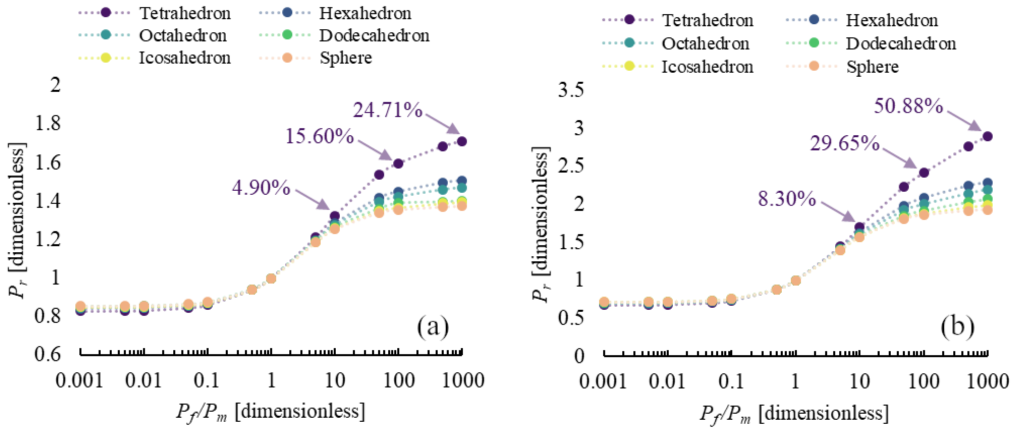

The impact of filler permeability relative to the polymer permeability, P_f/P_m, on the permeability of MMM for loading fraction, ϕ equal to (a) 10% and (b) 20%.

Results & Discussion

Ideal MMMs

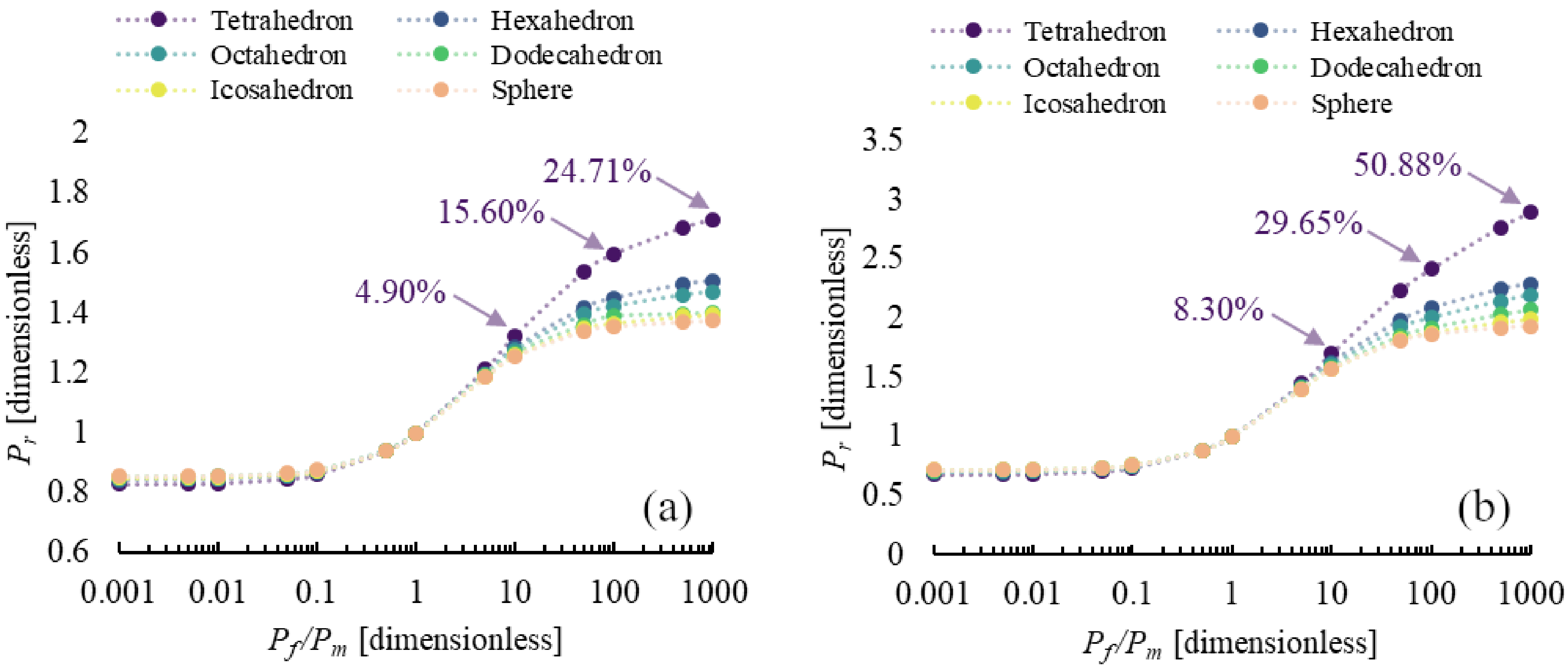

The impact of filler permeability relative to the polymer permeability, P_f/P_m, on the permeability of MMM for loading fraction, ϕ equal to (a) 10% and (b) 20%.

Results & Discussion

Ideal MMMs

- Impact of particle shape
- Impact of loading
- Impact of filler to polymer permeability ratio

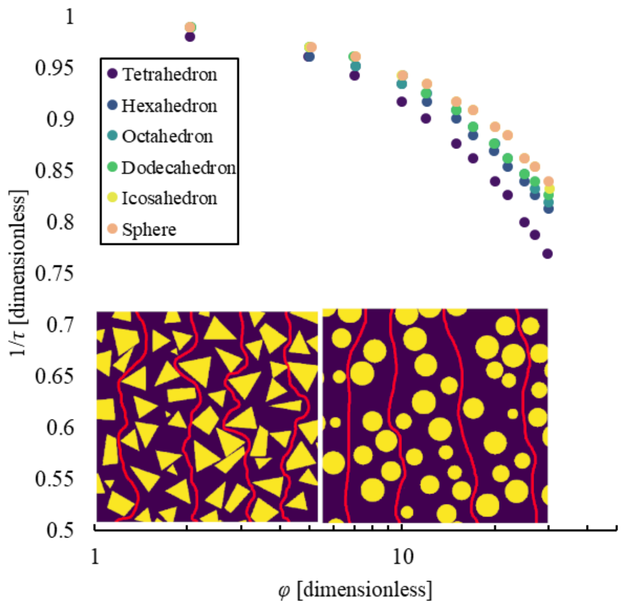

Comparison of the inverse of tortuosity (1/τ) of Platonic particles and spheres for loading.

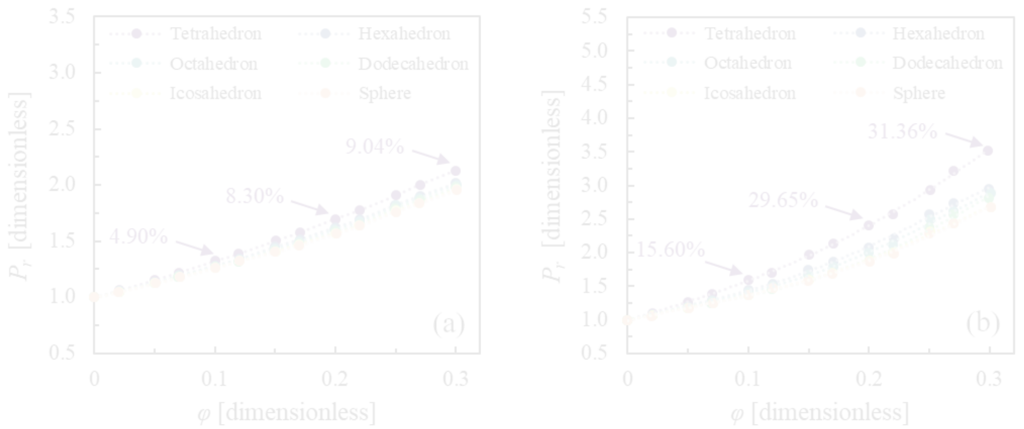

The impact of loading fractions, ϕ on the permeability of the MMM containing filler particles with a Platonic structure, as compared to spherical particles, for P_f/P_m is equal to (a) 10 and (b) 100.

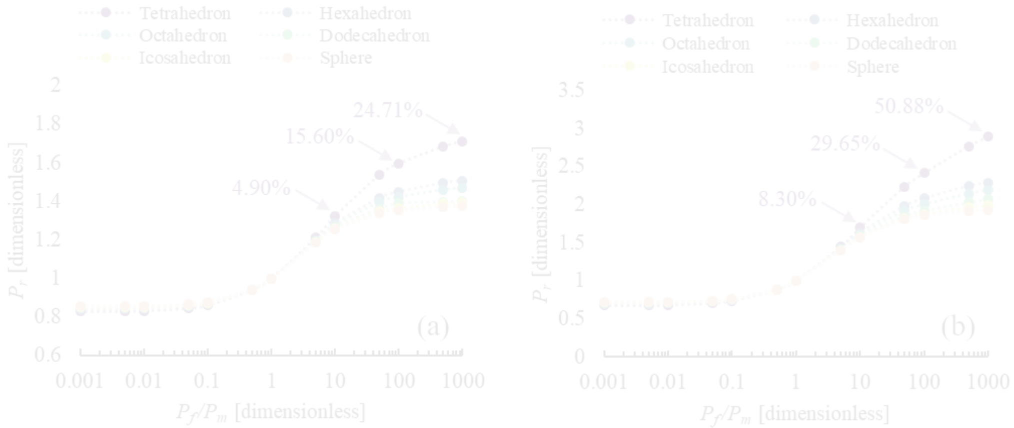

The impact of filler permeability relative to the polymer permeability, P_f/P_m, on the permeability of MMM for loading fraction, ϕ equal to (a) 10% and (b) 20%.

Results & Discussion

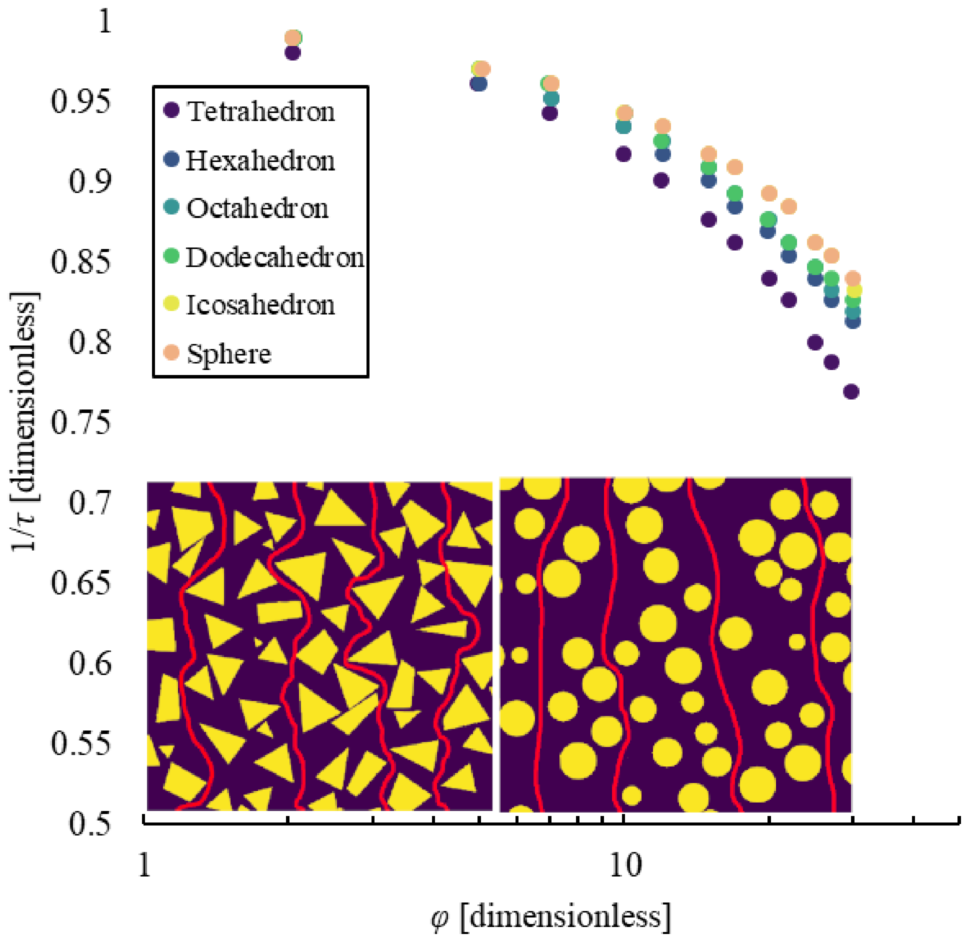

Comparison of the inverse of tortuosity (1/τ) of Platonic particles and spheres for loading fractions.

Results & Discussion

Ideal MMMs

- Impact of particle shape
- Impact of loading
- Impact of filler to polymer permeability ratio

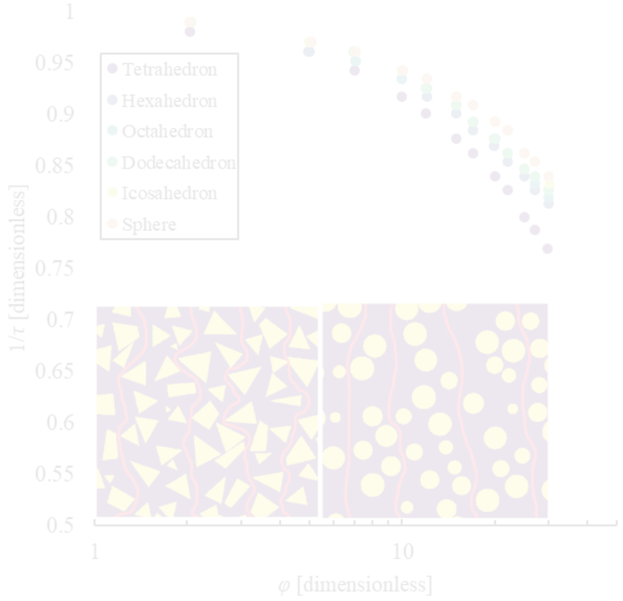

Comparison of the inverse of tortuosity (1/τ) of Platonic particles and spheres for loading fractions obtained by open-source MATLAB code, TauFactor [14].

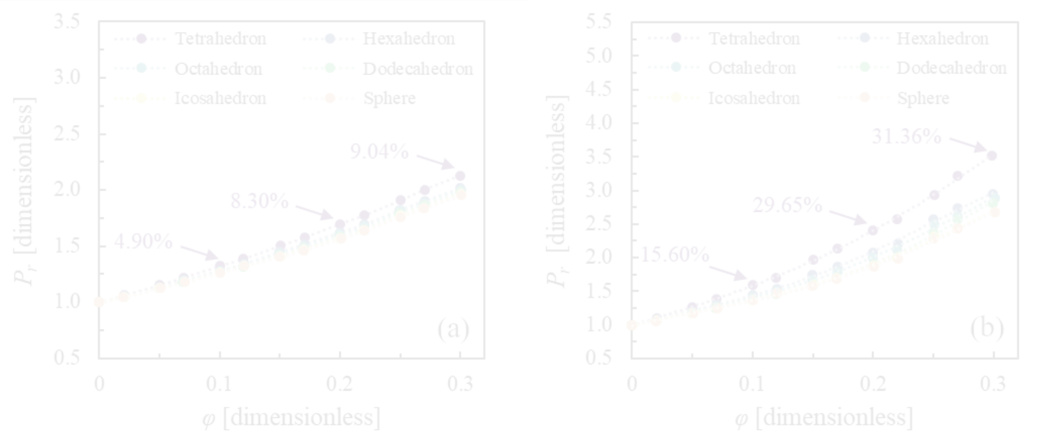

The impact of loading fractions, ϕ on the permeability of the MMM containing filler particles with a Platonic structure, as compared to spherical particles, for *P*f /*P*m is equal to (a) 10 and (b) 100.

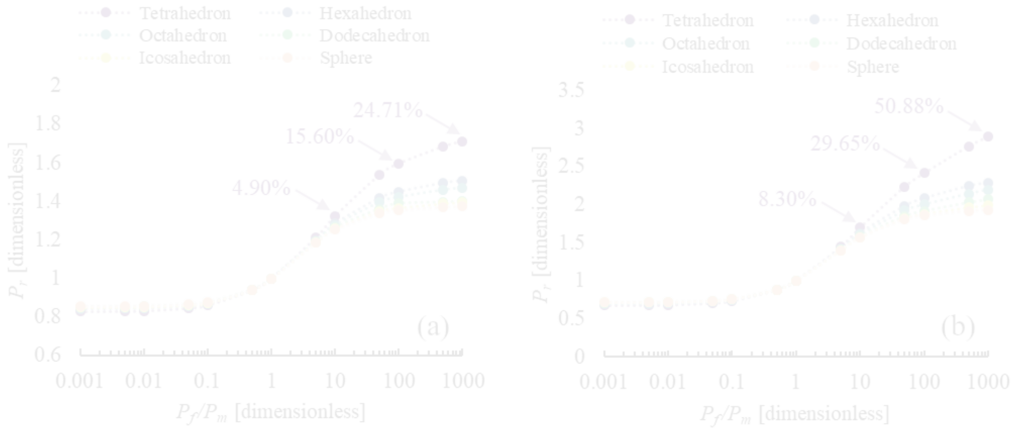

The impact of filler permeability relative to the polymer permeability, *P*f /*P*m, on the permeability of MMM for loading fraction, ϕ equal to (a) 10% and (b) 20%.

Results & Discussion

Ideal MMMs

- Impact of sphericity on the selectivity increase
- Impact of sphericity on the most compatible permeability between filler and polymer.

$$\boxed{\gamma_1 = \frac{P_{1,f}}{P_{1,m}}} \quad \boxed{\gamma_2 = \frac{P_{2,f}}{P_{2,m}}}$$

<u>perm-ratio</u>

$$\boxed{\alpha_m = \frac{P_{1,m}}{P_{2,m}}} \quad \boxed{\alpha_f = \frac{P_{1,f}}{P_{2,f}}}$$

<u>perm-selectivity</u>

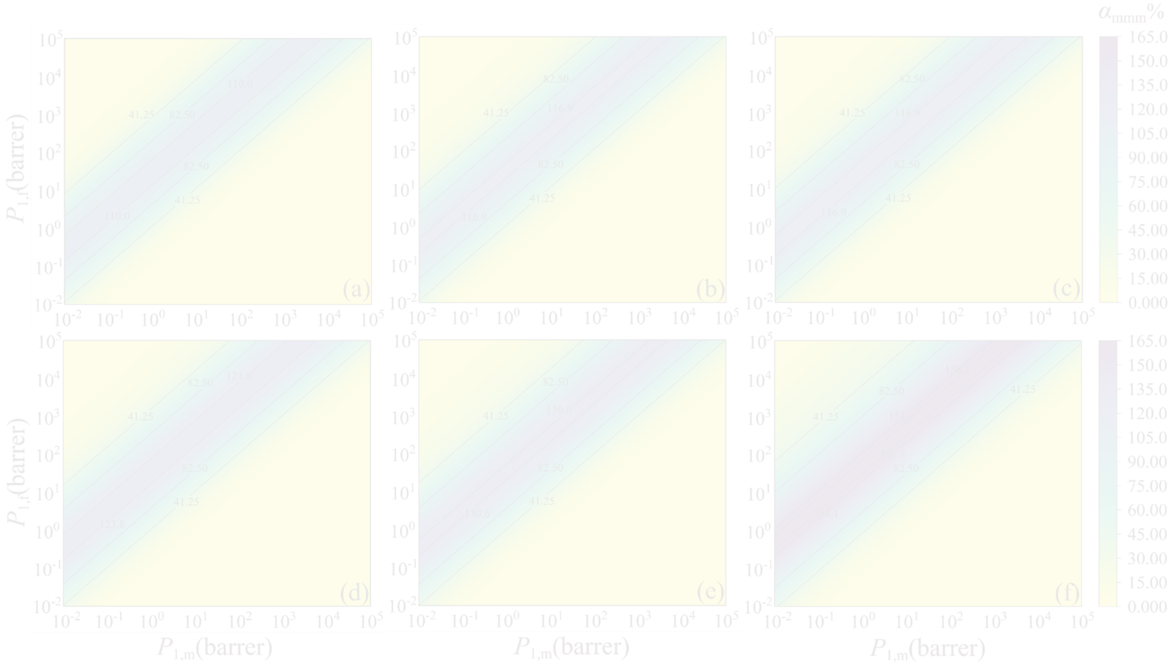

Colour maps indicating the percentage increase in MMM selectivity for various particle shapes of (a) sphere, (b) icosahedral, (c) dodecahedral, (d) octahedral, (e) hexahedral, and (f) tetrahedral.

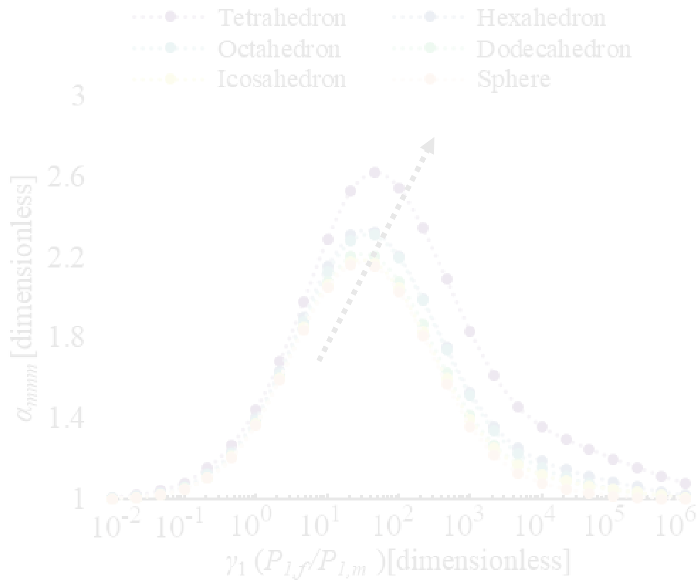

The MMM selectivity for a wide range of perm-ratio of faster gas ($P_{1,f}$ vs. $P_{1,m}$) at constant polymer perm-selectivity of α_m = 1 and filler permselectivity of α_f = 200 when the filler loading is ϕ=20% for all studies filler particle shapes.

Results & Discussion

Ideal MMMs

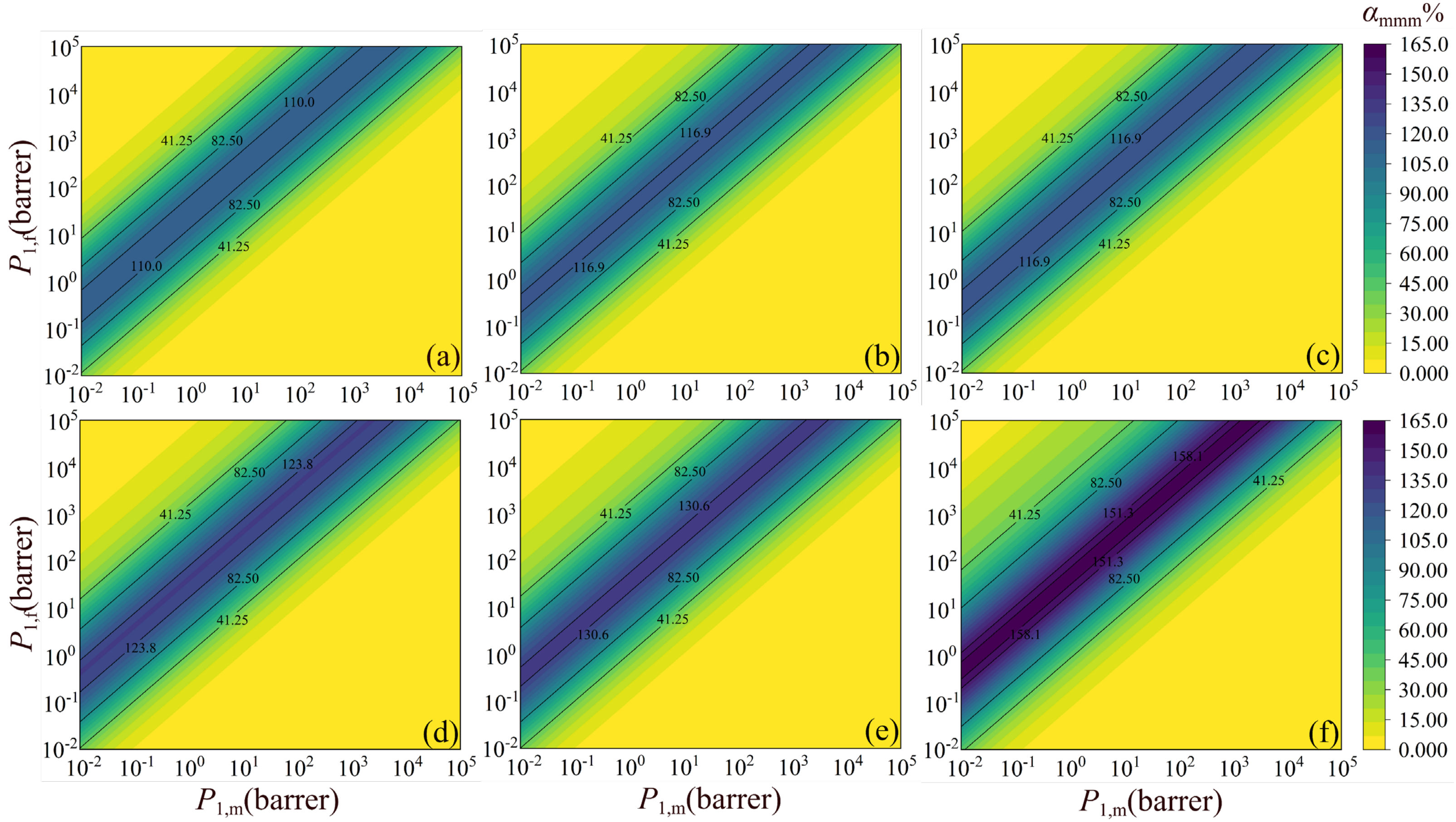

Color maps indicating the percentage increase in MMM selectivity for various particle shapes of (a) sphere, (b) icosahedral, (c) dodecahedral, (d) octahedral, (e) hexahedral, and (f) tetrahedral.

Results & Discussion

Ideal MMMs

- Impact of sphericity on the selectivity increase
- Impact of sphericity on the most compatible permeability between filler and polymer.

$$\gamma_1 = \frac{P_{1,f}}{P_{1,m}} \quad \gamma_2 = \frac{P_{2,f}}{P_{2,m}}$$

perm-ratio

$$\alpha_m = \frac{P_{1,m}}{P_{2,m}} \quad \alpha_f = \frac{P_{1,f}}{P_{2,f}}$$

perm-selectivity

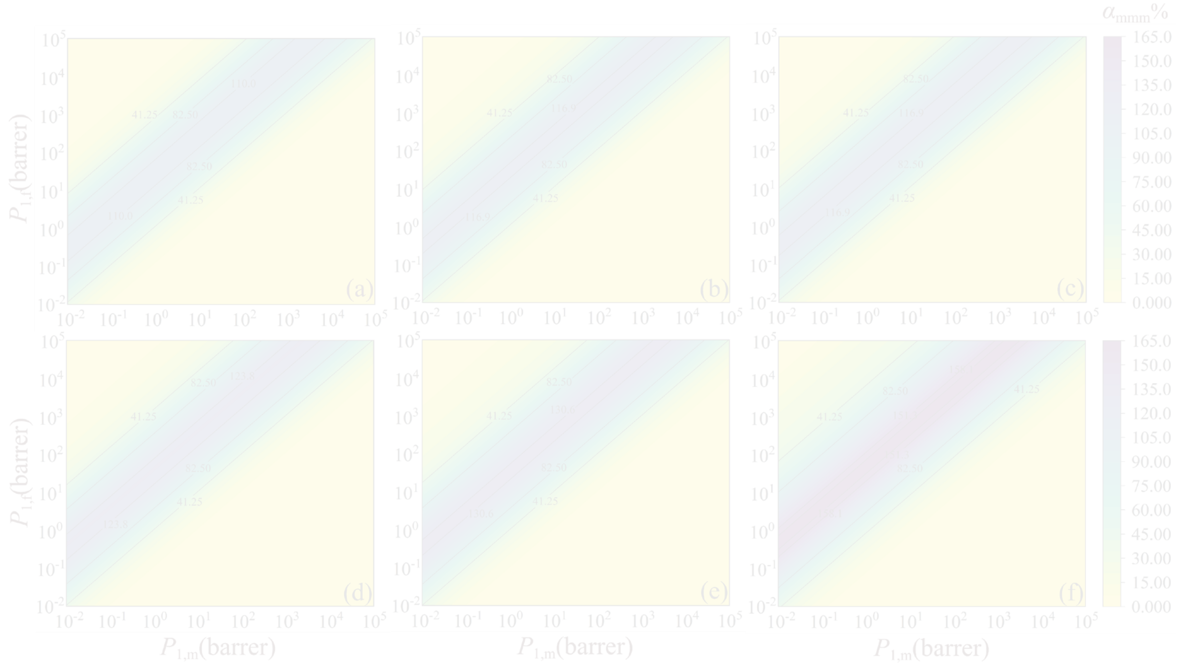

Colour maps indicating the percentage increase in MMM selectivity for various particle shapes of (a) sphere, (b) icosahedral, (c) dodecahedral, (d) octahedral, (e) hexahedral, and (f) tetrahedral.

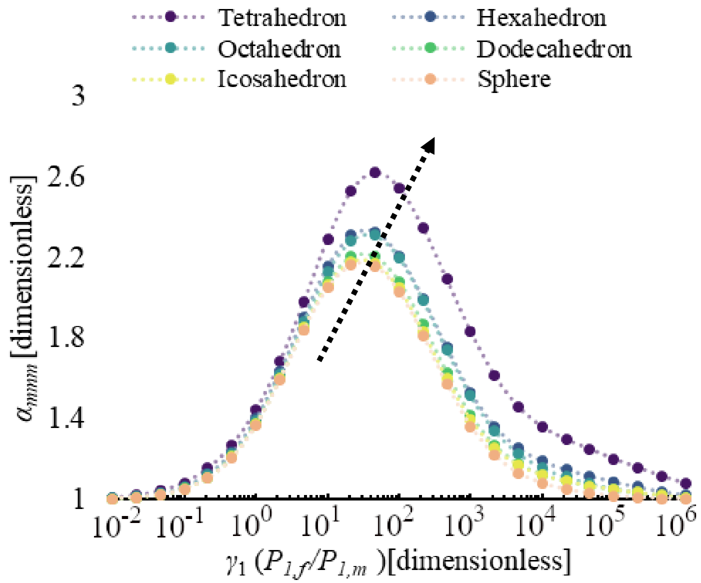

The MMM selectivity for a wide range of perm-ratio of faster gas ($P_{1,f}$ vs. $P_{1,m}$) at constant polymer perm-selectivity of α_m = 1 and filler permselectivity of α_f = 200 when the filler loading is ϕ=20% for all studies filler particle shapes.

Results & Discussion

Ideal MMMs

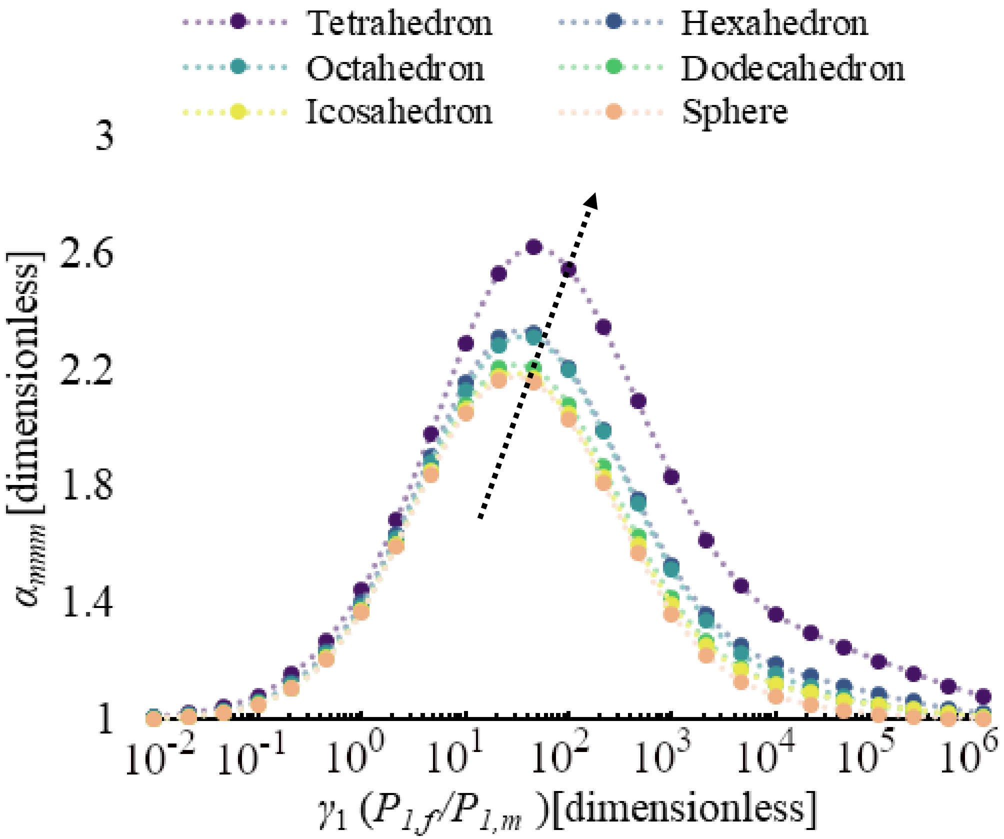

The MMM selectivity for a wide range of perm-ratio of faster gas ($P_{1,f}$ vs. $P_{1,m}$) at constant polymer perm-selectivity of $\alpha_m = 1$ and filler permselectivity of $\alpha_f = 200$ when the filler loading is $\phi = 20\%$ for all studies filler particle shapes.

Results & Discussion

Non-Ideal MMMs

- Impact of particle arrangements
- Impact of interface permeability
- Impact of filler loading of 8 and 15%

The flux intensity for various filler particle arrangements with particle shapes of (a–d)spherical and (e–h) tetrahedral.

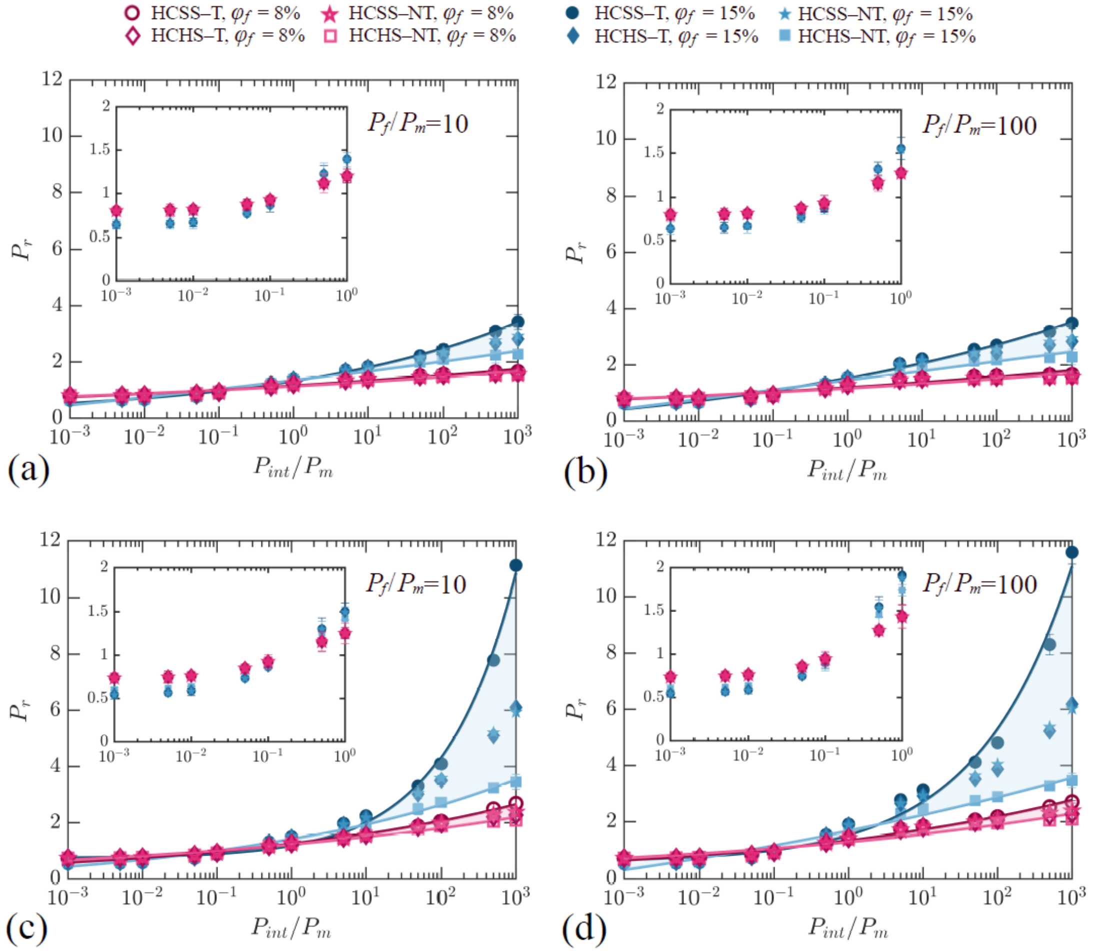

Impact of defect types on P_{eff} for different filler shapes — (a, b) spherical and (c, d) tetrahedral — is evaluated by examining variations in P_{int}.

Results & Discussion

Non-Ideal MMMs

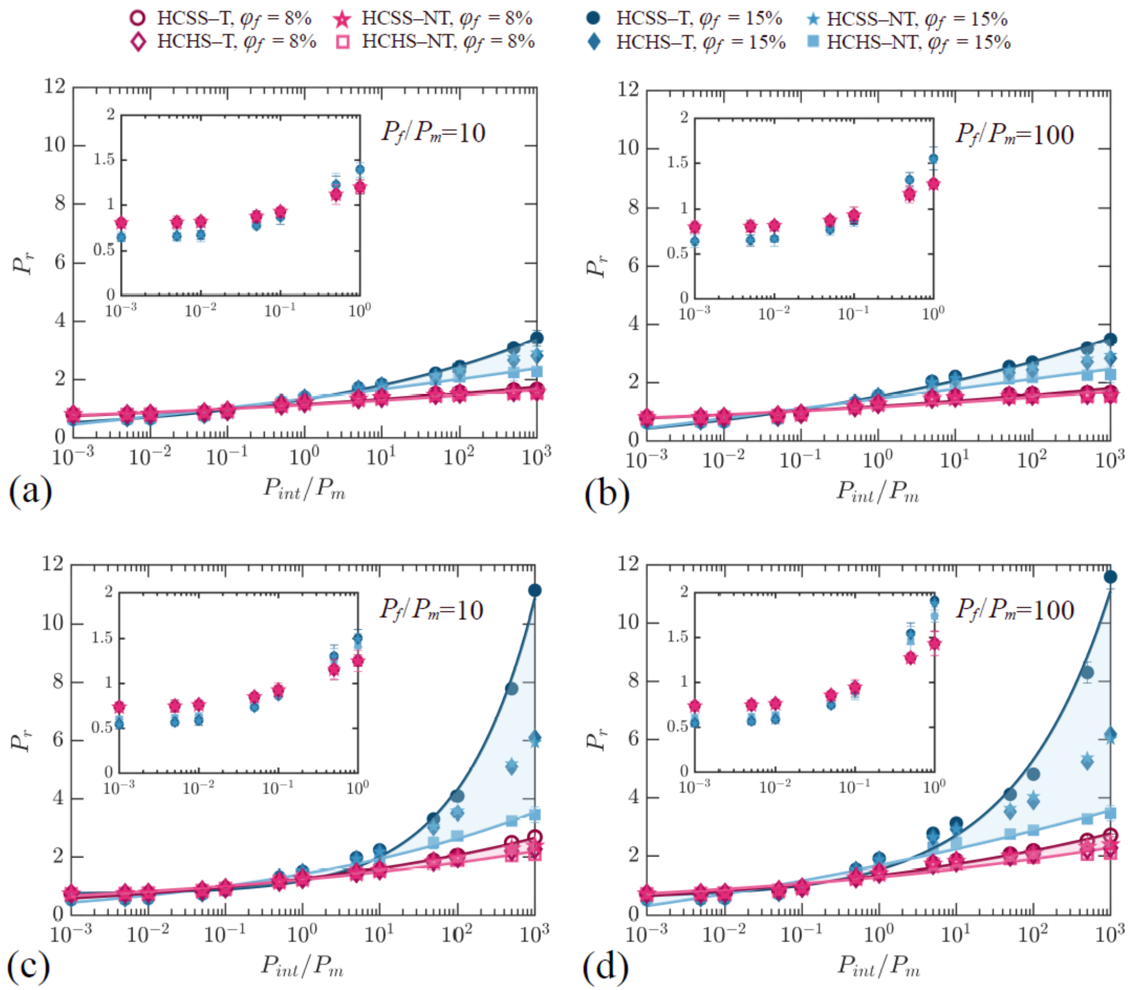

Impact of defect types on P_{eff} for different filler shapes — (a, b) spherical and (c, d) tetrahedral — is evaluated by examining variations in P_{int}.

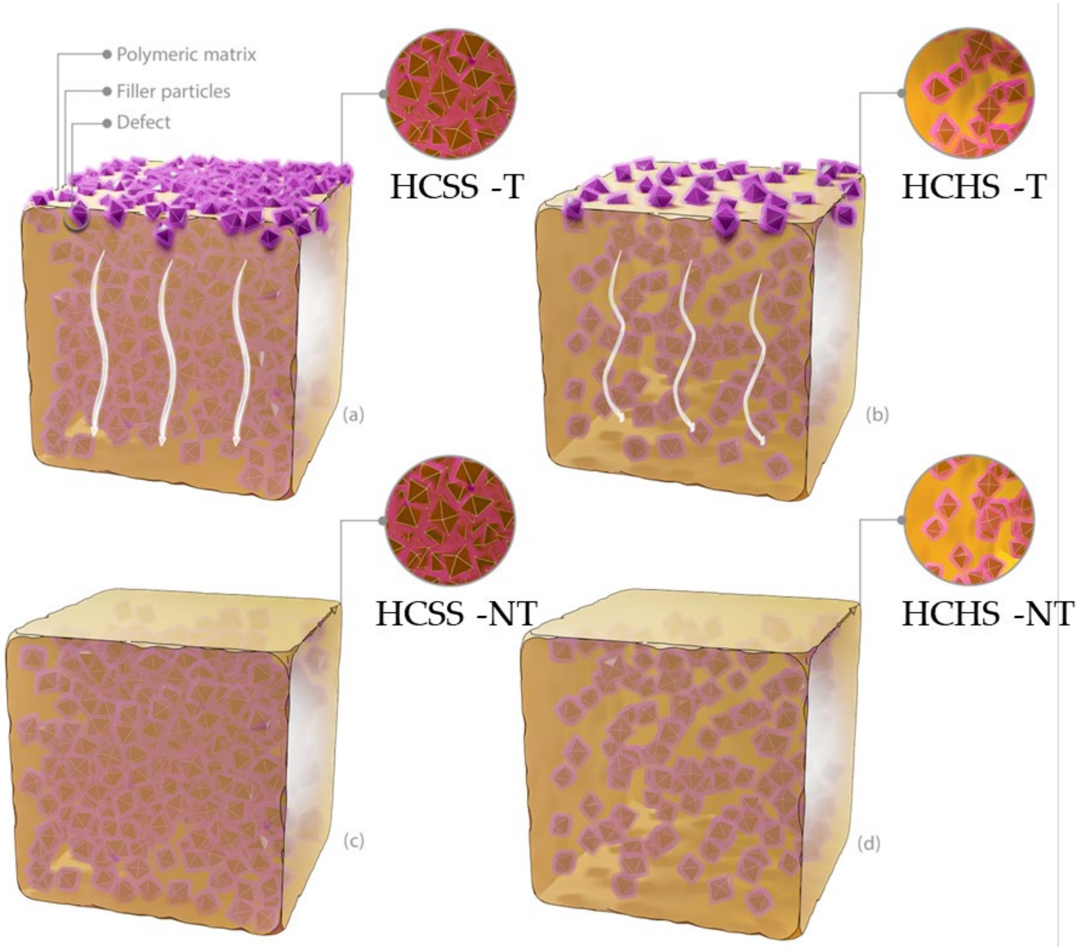

Results & Discussion

Non-Ideal MMMs

- Impact of interface permeability

$$\gamma_1 = \frac{P_{1,f}}{P_{1,m}} \quad \gamma_2 = \frac{P_{2,f}}{P_{2,m}}$$

perm-ratio

$$\alpha_m = \frac{P_{1,m}}{P_{2,m}} \quad \alpha_f = \frac{P_{1,f}}{P_{2,f}}$$

perm-selectivity

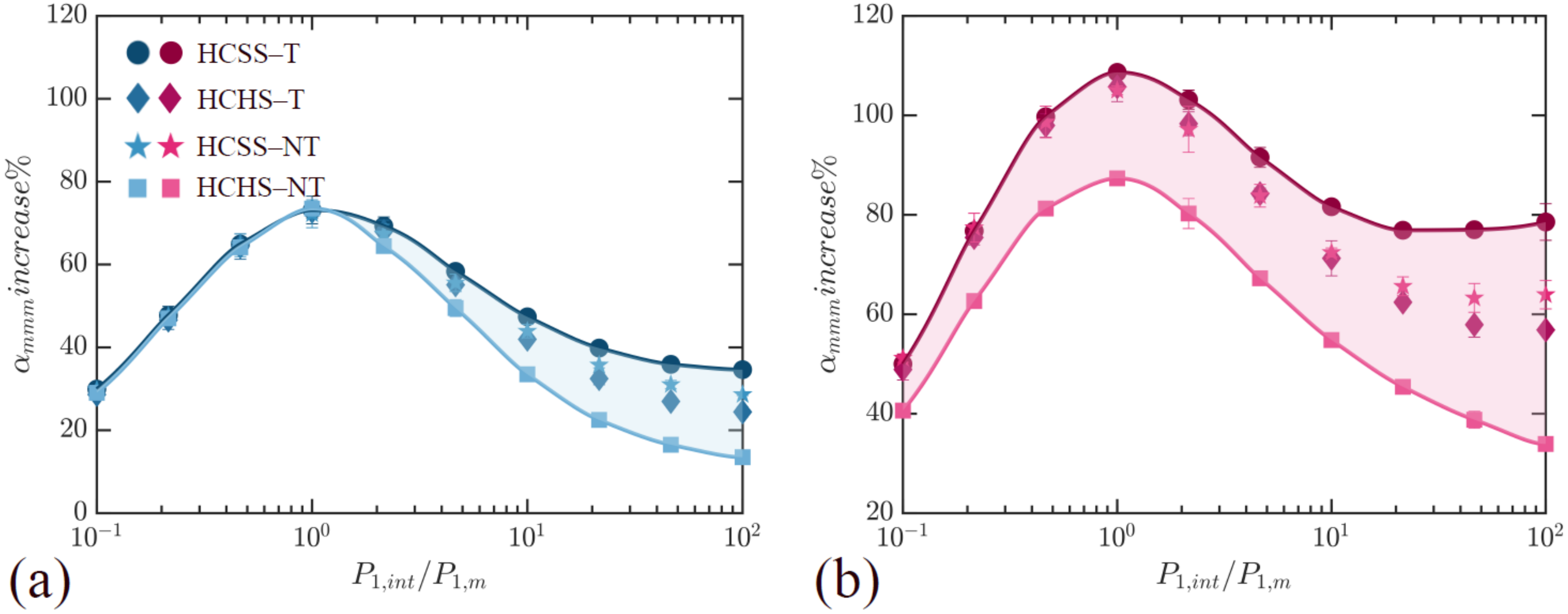

Impact of the perm-ratio of the faster gas in the defect region ($P_{1,\text{int}}/P_{1,\text{m}}$) on the percentage increase in αmmm for (a) spherical and (b) tetrahedral filler particles

Results & Discussion

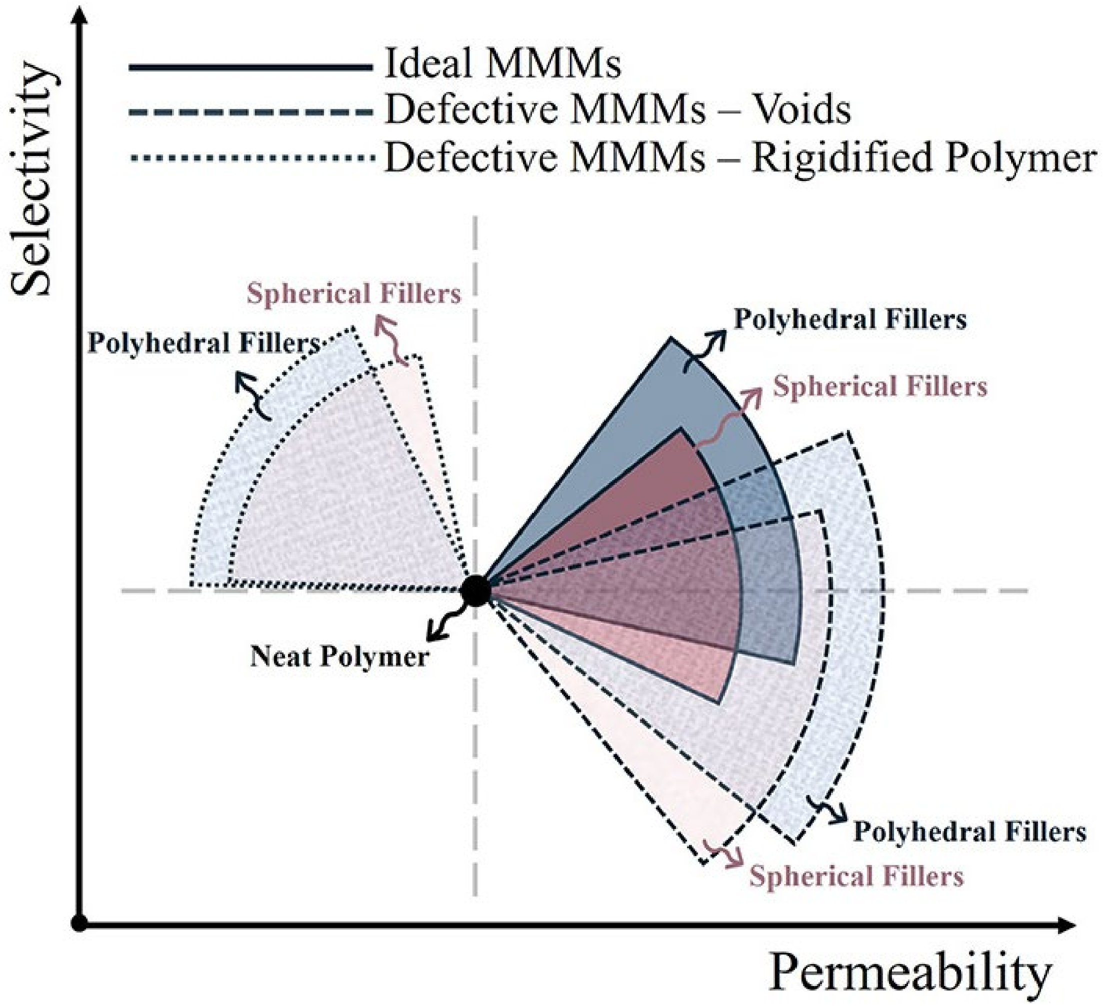

Conclusions & future works

01 Platonic particles with lower sphericity can effectively improve the permeability of MMMs compared to the spherical fillers.

02 At higher filler-to-polymer permeability ratios, a higher effective permeability is achieved with low-sphericity particles.

03 The impact of particle shape becomes more pronounced at higher loading fractions and filler-to-polymer permeability ratios.

04 The lower sphericity in particles leads to higher MMM selectivity at a comparable perm-ratio of faster gas.

05 Assessing gas transport in MMMs through integrating voxelized structures is an efficient approach for studying geometric factors that influence MMM performance

06 Arrangement of filler particles, and the overlap of defect regions are two key sources of uncertainty in predicting membrane permeability and selectivity.

07 The impact of interface thickness and filler volume fraction on membrane performance should be evaluated with consideration of filler shape.

08 The accurate characterisation of the polymer-filler interface's incompatibility and its impact on the performance of MMMs extends beyond the scope of empirical predictive models or methods relying solely on experimentally derived fitting parameters.

09 The impact of filler particle arrangement within the polymeric matrix, along with the associated defect shapes and structures, can be accurately and effectively captured by integrating voxelised structures into our computational framework.

Conclusions & future works

01 Platonic particles with lower sphericity can effectively improve the permeability of MMMs compared to the spherical fillers.

02 At higher filler-to-polymer permeability ratios, a higher effective permeability is achieved with low-sphericity particles.

03 The impact of particle shape becomes more pronounced at higher loading fractions and filler-to-polymer permeability ratios.

04 The lower sphericity in particles leads to higher MMM selectivity at a comparable perm-ratio of faster gas.

05 Assessing gas transport in MMMs through integrating voxelized structures is an efficient approach for studying geometric factors that influence MMM performance

06 Arrangement of filler particles, and the overlap of defect regions are two key sources of uncertainty in predicting membrane permeability and selectivity.

07 The impact of interface thickness and filler volume fraction on membrane performance should be evaluated with consideration of filler shape.

08 The accurate characterisation of the polymer-filler interface's incompatibility and its impact on the performance of MMMs extends beyond the scope of empirical predictive models or methods relying solely on experimentally derived fitting parameters.

09 The impact of filler particle arrangement within the polymeric matrix, along with the associated defect shapes and structures, can be accurately and effectively captured by integrating voxelised structures into our computational framework.

Thanks for your attention.